JGR Oceans

RESEARCH ARTICLE
10.1029/2021JC017518

Key Points:

- Understanding the simultaneous effects of tributary flows and lake intrusions is crucial to comprehend the dynamics of freshwater estuaries
- Circulation, thermal regime, wave action, and sediment transport depend on meteorological forcing, tributary flows, and lake intrusions
- The stage is set to apply this approach to study biogeochemical processes in lakes and estuaries

Supporting Information:

Supporting Information may be found in the online version of this article.

Correspondence to:

H. R. Bravo,
hrbravo@uwm.edu

Citation:

Khazaei, B., Bravo, H. R., Anderson, E. J., & Klump, J. V. (2021). Development of a physically based sediment transport model for Green Bay, Lake Michigan. *Journal of Geophysical Research: Oceans*, *126*, e2021JC017518. https://doi.org/10.1029/2021JC017518

Received 17 MAY 2021
Accepted 19 SEP 2021

© 2021. American Geophysical Union. All Rights Reserved.

Development of a Physically Based Sediment Transport Model for Green Bay, Lake Michigan

Bahram Khazaei[1,2], Hector R. Bravo[1], Eric J. Anderson[3,4], and Jeffrey V. Klump[5]

[1]Department of Civil and Environmental Engineering, University of Wisconsin-Milwaukee, Milwaukee, WI, USA, [2]Research Applications Laboratory, National Center for Atmospheric Research, Boulder, CO, USA, [3]Great Lakes Environmental Research Laboratory, National Oceanic and Atmospheric Administration, Ann Arbor, MI, USA, [4]Department of Civil and Environmental Engineering, Colorado School of Mines, Golden, CO, USA, [5]School of Freshwater Sciences, University of Wisconsin-Milwaukee, Milwaukee, WI, USA

Abstract Green Bay is the largest freshwater estuarine system on earth, drains one-third of the Lake Michigan basin and delivers one-third of the lake's phosphorus load. Southern Green Bay is a designated area of concern due to ecosystem degradation that includes eutrophication, harmful algal blooms, hypoxia, lost or altered habitat, and reduced water quality. While marine estuaries are subject to tidal influence and saltwater intrusion, this freshwater estuary is subject to lake intrusion of freshwater with different quality parameters. Understanding the simultaneous effects of tributary flows and lake intrusions is crucial to comprehend the dynamics of freshwater estuaries. A single hydrodynamic, wind-wave, and sediment transport model was developed for the lake and its estuary. This approach provides fine resolution in the estuary and simulates directly the combined effects of tributary flows and lake intrusions. The approach overcomes open-boundary limitations of nested models, and of whole-lake models that lack sufficient resolution or wind-wave and sediment transport simulation. The model confirms findings of previous studies and demonstrates how the circulation, thermal regime, wave action, and sediment transport in the estuary depend on meteorological forcing, tributary flows, and lake intrusions. The stage is set to apply this approach to study biogeochemical processes in lakes and estuaries.

Plain Language Summary Green Bay is a unique ecosystem located in the largest freshwater system on earth, the Laurentian Great Lakes. Almost one-third of tributary waters to Lake Michigan flow through Green Bay. Human activities in the watershed produce excessive amounts of contaminated and/or nutrient-rich sediments that are discharged to the bay. Sediments are not efficiently transported to Lake Michigan due to physical conditions in Green Bay, leading to ecosystem degradation, environmental and public health risks. We studied the movement, transport, and fate of sediments in Lake Michigan, with a special attention to Green Bay, by developing a physically based, 3D sediment transport model. This model development effort helps to predict circulation of contaminants and nutrients that are attached to the sediments, their settlement and burial, and the detachment from the bottom during storm events. The knowledge gained in this study will enhance our understanding of water quality conditions and nutrient recycling in freshwater estuaries, and will improve future restoration efforts and management plans.

1. Introduction

Green Bay is the largest freshwater estuarine system on earth, drains one-third of Lake Michigan basin and delivers one-third of the lake's total phosphorus load (Klump et al., 2018). The International Joint Commission designated southern Green Bay as an area of concern (AOC) in the 1980s due to several instances of ecosystem degradation including (but not limited to) eutrophication, harmful algal blooms (HABs), hypoxia, lost or altered habitat, and reduced water quality.

Green Bay has stimulated a significant amount of widely relevant research on the fate and behavior of toxics, biogeochemistry, habitat, biodiversity, and ecological processes. In particular, previous research relevant to hydrodynamics and sediment transport in Green Bay includes studies carried out on Green Bay, studies done on Lake Michigan and the Laurentian Great Lakes watershed, and studies done on marine estuaries. We will first concisely list those previous studies, then briefly explain how the present study differs

in geophysical terms, present the focus and goals of this research, and describe its place within current research needs in Green Bay.

Relevant previous research to hydrodynamics and sediment transport in Green Bay include studies on sediment resuspension and particle settling velocities (Eadie et al., 1991), measurement of horizontal sediment transport (Hawley & Niester, 1993), on patterns of mass sedimentation and of deposition of sediment contaminated by PCBs (Manchester-Neesvig et al., 1996), on sedimentary phosphorus (Klump et al., 1997), modeling hydrodynamics, sediment transport and sorbent dynamics (HydroQual Inc., 1999), on benthic carbon and nitrogen mass balances (Klump et al., 2009), explaining the role of circulation and heat fluxes in the formation of stratification leading to hypoxia in Green Bay (Hamidi et al., 2015), a biogeochemical analysis of hypoxia in Green Bay (Labuhn, 2017), analysis of the physical drivers of the circulation and thermal regime impacting seasonal hypoxia in the bay (Bravo et al., 2017), satellite-based estimations of surficial sediment transport (Hamidi et al., 2017), quantifying the influence of cold-water intrusions in Green Bay (Grunert et al., 2018), and estimation of transport timescales (Bravo et al., 2020). Previous relevant research done on Lake Michigan and the Laurentian Great Lakes watershed include studying influences of suspended sediments on the ecosystem in Lake Michigan (Chen et al., 2004; Ji et al., 2002), observations of sediment transport in Lake Erie (Hawley & Eadie, 2007), analysis of sediment resuspension mechanisms and their contributions to high-turbidity events in Lake Erie (Niu et al., 2018; Valipour et al., 2017), 3D coupled bio-physical modeling experiments on the St. Clair River, Lake St. Clair, and Detroit River System (Anderson et al., 2010) and Lake Erie (Lin et al., 2021; Valipour et al., 2016), relationships between wind-driven and hydraulic flow in Lake St. Clair and the St. Clair River Delta (Anderson & Schwab, 2011), simulating a phytoplankton bloom in Lake Michigan using a coupled physical-biological model (Luo et al., 2012), predicting the oscillating bi-directional exchange flow in the Straits of Mackinac (Anderson & Schwab, 2013), modeling the climatology of seasonal general circulation and thermal structure in the Great Lakes (Bai et al., 2013), modeling the effect of invasive quagga mussels on the spring phytoplankton bloom in Lake Michigan (Rowe et al., 2015), investigating the thermal response to meteorological forcing in a hydrodynamic model of Lake Superior (Xue et al., 2015), modeling *Escherichia coli* at Beaches in Southern Lake Michigan (Safaie et al., 2016), modeling of dreissenid mussel impacts on Lake Michigan (Shen, 2016), modeling wind-waves from deep to shallow waters in Lake Michigan (Mao & Xia, 2017), biophysically modeling the influence of invasive quagga mussels, phosphorus loads, and climate on spatial and temporal patterns of productivity in Lake Michigan (Rowe et al., 2017), a study on the dynamics of wave-current-surge interactions in Lake Michigan (Mao & Xia, 2020), and an investigation of the drivers of warmings in deep-waters of Lake Michigan (Anderson et al., 2021).

There is vast research on marine estuaries, so we will just mention as examples the book *Estuarine Ecohydrology* by Wolanski and Elliott (2015), a study on the impact of tides and winds on estuarine circulation in the Pearl River Estuary (Lai et al., 2018), a study on the influence of suspended sediment front on nutrients and phytoplankton dynamics off the Changjiang Estuary (Ge et al., 2020), and an article on estuarine ecohydrology study of sediment transport in coastal zones by (Ouillon, 2018). Wolanski and Elliott (2015) defined an estuary as a semi-enclosed body of water connected to the sea as far as the tidal limit or the salt intrusion limit and receiving freshwater runoff, recognizing that the freshwater inflow may not be perennial (i.e., it may occur only for part of the year) and that the connection to the sea may be closed for part of the year (e.g., by a sand bar), and that the tidal influence may be negligible. Sediments determine the estuarine bed habitats (i.e., the fundamental niche for the fauna and flora on the bottom) and they influence organisms in the water column. Sediments are mobile and their dynamics occur at time scales of millennia, of intermediate timescales due to the tides, of storms, of river floods, of the seasons, and of turbulence.

The Green Bay estuary is a semi-enclosed body of water connected to the freshwater Lake Michigan as far as the limit of lake intrusion and receiving freshwater runoff. The circulation, thermal regime, wave regime, and sediment transport in Lake Michigan and its Green Bay estuary are driven by the momentum flux generated by wind, the heat flux across the water surface, the Earth's rotation, thermal stratification, and topography (Bravo et al., 2017). While marine estuaries are subject to tidal influence and saltwater intrusion, in freshwater estuaries like Green Bay, the tidal influence is relatively smaller and salinity effects are nonexistent. The role of the large receiving and exchanging large body of water is played by lake water intrusion of currents, waves, and transport of waters with very different quality parameters such as density,

temperature, and conductivity. Understanding the simultaneous effects of tributary flows and lake water intrusions is vital to comprehend the dynamics of freshwater estuaries.

Previous hydrodynamic and transport modeling of Green Bay was done either by employing nested models of the bay that represent the exchange of mass, energy, and momentum with Lake Michigan using potentially problematic open boundary conditions, generally obtained from low-resolution lake models (Hamidi et al., 2015; HydroQual Inc., 1999), or else using whole-lake models that lack the desired high resolution in the bay (Lee et al., 2005, 2007; Lou et al., 2000; Mao & Xia, 2017; Rowe et al., 2015, 2017; Safaie et al., 2016; Shen, 2016). The study presented herein bypasses the use of open boundary conditions by developing a single hydrodynamic, wave, and sediment transport model of the lake that has high resolution in the bay and in the exchange zone between the open lake and the bay.

The purposes of this research were to: (a) use the existing database of hydrodynamic, wave, and sediment field data to develop a predictive model of sediment transport in Lake Michigan, with an emphasis on Green Bay; (b) use the sediment transport model to contribute to understanding ecological and environmental problems in the bay, and to recommend long-term solutions; and (c) analyze summertime patterns of circulation, wave action, current and wave-induced bottom shear stress, thermal structure, and sediment transport in Lake Michigan, with special attention to Green Bay. The sediment transport model is designed to be a compatible component of the NOAA Lake Michigan-Huron Operational Forecast System (LMHOFS) for future water quality and shoreline protection applications for Lake Michigan and other Great Lakes.

Green Bay represents a true "proving ground" for adaptive restoration. Among the main recommendations of a recent summit on the "Ecological and Socio-Economic Tradeoffs of Restoration in the Green Bay Ecosystem" was the creation of a "Green Bay Ecosystem Simulation and Data Consortium" serving as a data clearing house, building upon the significant progress to date, and developing a modeling framework and visualization tools, furthering public outreach efforts, and ensuring a sustained growth in scientific expertize (Klump et al., 2018). Gaps in biogeochemistry and hydrodynamics identified during the restoration summit include incorporation of wind-wave models and an understanding of resuspension and its role in carbon and phosphorus cycling, the delineation of diagenetic versus rapid carbon remineralization and its influence on sediment and water column respiration, the role of denitrification and nitrogen-fixation in the overall nitrogen budget for the bay and its link to nutrient stoichiometry and phytoplankton and cyanobacterial production. Extending models to multiple-year simulations, linking to refined watershed models, and engaging a complete range of downscaled regional climate scenarios to assess the magnitude of projected variability for the 21st century are necessary to provide more robust projections and guide expectations for adaptive management efforts (Klump et al., 2018). The present study addressed the incorporation of physical processes including wind-wave dynamics and sediment transport, will be used to extend models to multiple-year simulations, will engage downscaled regional climate scenarios to assess variability during the 21st century, and sets the stage for future work on other biogeochemical modeling gaps listed above.

2. Model Components and Formulation

Physically based sediment transport modeling is essential in Green Bay due to complicated conditions of the system dynamics. Previous efforts intended to understand physical processes and particle dynamics in Green Bay faced obstacles in model development. Major obstacles included the use of Cartesian structured rectangular grids in POM-based models that limits the representation of small-scale shoreline features in Green Bay, and difficulties in modeling thermal structures and stratified flows in the shallow estuarine systems, especially during upwelling or downwelling events. Challenges in the implementation of Environmental Fluid Dynamics Code (EFDC) models were difficult documentation and neglected wind-wave effects. Additionally, those models are computationally expensive and not very efficient if a high-resolution grid in a large domain such as Lake Michigan is implemented.

To overcome those obstacles, a state-of-the-art modeling approach, the Finite-Volume Community Ocean Model (FVCOM) was used in this research. FVCOM's features such as the use of an unstructured-grid solver and a parallel mode computation option make it a suitable candidate for the Green Bay sediment transport model. FVCOM is also equipped with several water quality tools that can integrate different physical and biogeochemical processes and enhance the implementation of transport models in restoration applications.

2.1. Circulation Model: FVCOM

Developed by Chen et al. (2003), FVCOM is a free-surface, primitive-equation ocean model and is a powerful numerical solution of the conservation of mass, momentum, and energy principles that solves for currents, temperature, salinity, density, and other hydrodynamic variables in a 3D Cartesian grid space. FVCOM accounts for Coriolis effect and uses a modified MY-Level 2.5 turbulence closure scheme (Mellor & Yamada, 1982) for vertical mixing calculations and Smagorinsky's (1963) eddy scheme for horizontal mixing.

FVCOM has several features that make it an efficient computational tool for the physical modeling of large lakes. FVCOM runs based on unstructured sigma-coordinated (terrain-following) grids, in which the 3D domain is discretized into triangular finite volumes. That feature increases model flexibility in representing irregular geometry of shorelines in the Green Bay estuary and preserves fine features of several peninsulas and islands that restrict physical processes in the bay. Additionally, FVCOM is computationally efficient because it runs in parallel and also adopts a split mode numerical scheme, in which it first calculates the water surface elevation and depth-averaged currents in the external mode and then solves for the vertical diffusive transport in a 3D internal mode.

FVCOM has been successfully implemented in various hydrodynamic applications such as coastal modeling (e.g., Chen et al., 2003, 2007; Huang et al., 2008; B. Li et al., 2017; J. Li et al., 2018; Zhang et al., 2018), Great Lakes studies (e.g., Anderson & Schwab, 2011; Anderson et al., 2010; Bai et al., 2013; Mao et al., 2016; Mao & Xia, 2020; Read et al., 2010; Shore, 2009; Xue et al., 2015), and modeling rivers, straits, and channels (e.g., Anderson & Phanikumar, 2011; Anderson & Schwab, 2013; Guerra et al., 2017; Lai et al., 2018). It has also been coupled with water quality and biogeochemical models in various case studies (e.g., Luo et al., 2012; Rowe et al., 2015, 2017; Safaie et al., 2016; Shen, 2016). In this study, we used FVCOM version 4.1 to develop the physical circulation model of Lake Michigan.

2.2. Wave Model: FVCOM-SWAVE

Sediment movement is primarily due to advective-diffusive transport in the water column; however, sediment processes near the bottom are significantly affected by the wave interactions. Therefore, the implementation of wave actions in the sediment model is an important step toward simulations of more realistic current-wave-sediment interactions in the bottom boundary layer. Simulating WAves Nearshore (SWAN) model is adopted by FVCOM (FVCOM-SWAVE) as the wave simulator. SWAN was developed by Booij et al. (1999) and models wave evolution using transport equations to solve for wave action density N as follows:

$$\frac{\partial N}{\partial t}+\frac{\partial c_x N}{\partial x}+\frac{\partial c_y N}{\partial y}+\frac{\partial c_\sigma N}{\partial \sigma}+\frac{\partial c_\theta N}{\partial \theta}=\frac{S_w}{\sigma} \tag{1}$$

where N is the energy density E divided by the relative frequency σ, $N(\sigma,\theta)=E(\sigma,\theta)/\sigma$, (c_x, c_y) are the propagation velocities in the (x, y) Cartesian grid coordinates, σ and θ are the intrinsic wave frequency and direction, c_σ is the propagation velocity due to variations in depth and currents, c_θ is the propagation in wave direction, and S_w is acting as a source/sink term to represent the effects of wind-wave generation, energy dissipation due to whitecapping, depth-induced wave breaking, bottom friction, and nonlinear wave-wave interactions. Specific details of the SWAN model formulation and validation are described in the literature (Booij et al., 2004; Ris et al., 1999). SWAN is a structured-grid wave model and was converted to an unstructured-grid finite-volume model to be consistent with FVCOM (Chen et al., 2013; Qi et al., 2009).

SWAN has become popular in various applications including ocean wave simulations, engineering applications, modeling coastal and estuarine systems, and wave forecasting studies (Chen et al., 2018). SWAN is particularly adjusted for coastal regions with shallow waters, which makes it suitable for modeling sediment transport in Green Bay. Recent applications of the SWAN in studying Lake Michigan wave dynamics have also indicated good performance and applicability of the model for the Green Bay sediment transport studies (Mao et al., 2016; Mao & Xia, 2017).

2.3. Sediment Transport Model: FVCOM-SED

We used the FVCOM built-in sediment transport model (FVCOM-SED) in this study to model sediment processes in Green Bay and Lake Michigan. FVCOM-SED was developed based on the Community Sediment Transport Modeling Systems (CSTMS) by Warner et al. (2008) and was further modified to account for cohesive and mixed sediment dynamics (Sherwood et al., 2018). CSTMS was developed to be coupled with the structured-grid-based Regional Ocean Modeling System and was modified to be consistent with FVCOM unstructured-grid solver (Chen et al., 2013).

FVCOM-SED accounts for several sediment mechanisms including suspended and bedload transport, layered bed dynamics, and erosion/deposition actions for an unlimited number of cohesive and non-cohesive sediment classes. Each sediment class is characterized by mean grain diameter, particle density, settling rates, and bed erosion characteristics. Each bed layer is defined based on the bulk characteristics of sediment classes in that layer and its initial thickness. The FVCOM-SED version 4.1 was only able to initiate the sediment transport model based on the uniform distribution of sediment classes in the entire domain. That seems to be an unrealistic assumption for Lake Michigan sediment stratigraphy. Therefore, we updated the code so that the model can take user-defined non-uniform distribution of sediment classes in the bed layer (Khazaei, 2020, Appendix A).

Bed layer characteristics, in particular thickness, is immediately affected by sediment actions such as erosion and deposition. In order to keep the number of bed layers constant throughout the simulation, an active layer is considered on top of sediment layers. The thickness of this active layer (z_a) is calculated in each time step based on the Harris and Wiberg's (2001) formulation as follows:

$$z_a = \max\left[k_1\left(\tau_{\text{sf}} - \tau_{\text{ce}}\right), 0\right] + k_2 D_{50} \tag{2}$$

where τ_{sf} is the maximum bottom friction shear stress due to combined effects of currents and waves (N/m^2), τ_{ce} is the critical shear stress for erosion (N/m^2), D_{50} is the median grain diameter at the sediment-water interface (m), and k_1 and k_2 are empirical constants with values of 0.007 and 6.0, respectively. Sediment transport is limited to the mass available in the active layer in each time step.

The total load is the accumulated suspended load in the water column and bedload. FVCOM-SED calculates the suspended load by accounting for advective and diffusive concentration-based transport in the water column, as follows:

$$\frac{\partial C}{\partial t} + \frac{\partial uC}{\partial x} + \frac{\partial vC}{\partial y} + \frac{\partial wC}{\partial z} = \frac{\partial}{\partial x}\left(A_H \frac{\partial C}{\partial x}\right) + \frac{\partial}{\partial y}\left(A_H \frac{\partial C}{\partial y}\right) + \frac{\partial}{\partial z}\left(A_V \frac{\partial C}{\partial z}\right) + \frac{1}{H_z} C_{\text{Source/sink}} \tag{3}$$

where C is the suspended sediment concentration, (u, v, w) are the three components of currents in the (x, y, z) Cartesian grid space, A_H and A_V are the horizontal and vertical eddy viscosity, and H_z is the thickness of grid cells. $C_{\text{source/sink}}$ accounts for additional vertical transport mechanisms due to settling and resuspension:

$$C_{\text{source/sink}} = -\frac{\partial \omega C}{\partial S} + E_s \tag{4}$$

where ω is the settling velocity positive in the upwards direction (m/s) and E_s is the erosion rate (kg/m^2/s) in the vertical sigma coordinate direction S. Ariathurai and Arulanandan (1978) defined erosion rates of cohesive soils as a function of bed erodibility constant, sediment porosity (top layer sediment particles in this case), maximum bottom shear stress, and critical shear stress for erosion. Transport of suspended load is constrained to a zero-flux boundary condition at the surface of the water column and the net balance between erosion and deposition at the bottom.

While the suspended load includes the flux of sediment mass at the sediment-water interface and transport in the water column, the bedload is considered as the horizontal exchange within the top layer of the bed and is estimated based on the Hans Albert Einstein's definition of nondimensional volumetric sediment flux:

$$q_{\text{bl}} = q_{s*} D_{50} \sqrt{\left(s-1\right) g D_{50}} \tag{5}$$

where q_{bl} is the horizontal bedload transport rate (m^2/s) and $s = \rho_s/\rho_w$ is the specific density of sediments in the water. q_{s*} is the magnitude of the nondimensional transport rate and could be determined based on the Meyer-Peter and Müller's (1948) scheme.

Mixed-sediment bed processes occur when both cohesive and non-cohesive sediments are present and there is a considerable amount of mud (fine cohesive sediment) in the sediment layer (Mitchener & Torfs, 1996). FVCOM-SED (and CSTMS) adopts a method similar to Le Hir et al. (2011) and Mengual et al. (2017) to force resuspensions, in which mixed beds form when a mud content of 3%–30% is present in the sediment layer. Their strategy is tested and recommended for implementation in real case 3D hydro-sedimentary modeling applications. This approach means that in mixed-sediment bed conditions effective critical shear stress of the bottom ($\tau_{ce,eff}$) is calculated based on a weighted combination of critical shear stresses of cohesive and non-cohesive portions of the bed:

$$\tau_{ce,eff} = \max\left[P_c\tau_{cb} + \left(1 - P_c\right)\tau_{ce}, \tau_{ce}\right] \quad (6)$$

where τ_{ce} is the critical shear stress for each sediment class, τ_{cb} is the bulk critical shear stress for the sediment layer based on Sanford's (2008) approach, and P_c is the dimensionless cohesive behavior parameter. P_c is a function of the mud content in the bed layer with lower values denoting a non-cohesive behavior and vice versa. It is important to note that while the bed erodibility of non-cohesive sediment is treated as the property of individual sediment classes, the erodibility of cohesive sediment is treated as the bulk property of the bed. Following Sherwood et al. (2018), the equilibrium bulk critical shear stress $\tau_{cb,eq}$ is defined in terms of an exponential profile defined by a slope and offset:

$$\tau_{cb,eq} = a\exp\left[\frac{\ln\left(z_p\right) - \text{offset}}{\text{slope}}\right] \quad (7)$$

where z_p is mass depth defined as the cumulative dry mass of sediment overlying a given depth in the bed (kg/m^2) and $a = 1$ Pa m^2/kg is a dummy coefficient that produces the correct units of critical shear stress. The parameter values of $offset = 2\ \ln(kg/m^2)$, $slope = 5\ \ln(kg/m^2)$, and timescale for consolidation $T_c = 8$ hr were based on the recommendations of the CSTMS and FVCOM-SED settings.

FVCOM-SED is fully coupled with the FVCOM ocean model and FVCOM-SWAVE to account for the current-wave-sediment interactions (Chen et al., 2013). More details of the CSTMS model, mixed sediment transport mechanisms, and model validation are provided in the literature (Sherwood et al., 2018; Warner et al., 2008). In Section 3.3, we elaborate on the characterization of different sediment classes and their properties for the Lake Michigan sediment transport model.

3. Model Design

3.1. Study Area

While the focus of the current study is Green Bay, to avoid the uncertainty and difficulty of obtaining internal or open-lake boundary conditions at the connection straits with Lake Michigan, a whole-lake model is developed. Green Bay is 190 km long in its longest axis and, on average, is about 20 km wide. With an average and maximum depths of approximately 20 and 50 m, respectively, Green Bay is considered a shallow coastal water body. The maximum depth in Lake Michigan is about 280 m.

Chambers Island cross-section divides Green Bay into lower and upper sections. Lower Green Bay is the hotspot of environmental issues, where Fox River discharges runoff from the heavily developed and stressed Fox River watershed into the bay. The watershed is mostly covered by vegetated areas (Khazaei & Wu, 2018), and the cities of Appleton and Green Bay, large industrial sites, and farmlands impact the concentration and quality of particles running into the river (Klump et al., 1997; Velleux et al., 1995). The Fox River alone contributes about two-thirds of the nutrient and particulate tributary loading into Green Bay and almost one-third of the total phosphorus load to Lake Michigan (Harris & Christie, 1987). Figure 1 shows the location of Lake Michigan and Green Bay in the Great Lakes basin and Green Bay AOC.

3.2. Grid and Simulation Specifications

Circulation and transport mechanisms are very sensitive to the morphology of the system. Shallow waters and the complex geometry of the Green Bay shorelines require a fine grid that can resolve those detailed features (Figure S1). Long Tail Point and Little Tail Point Islands located on the western shore of lower Green Bay, Green and Chambers Islands in the central bay areas, as well as Plum, Detroit, Washington, Rock, St.

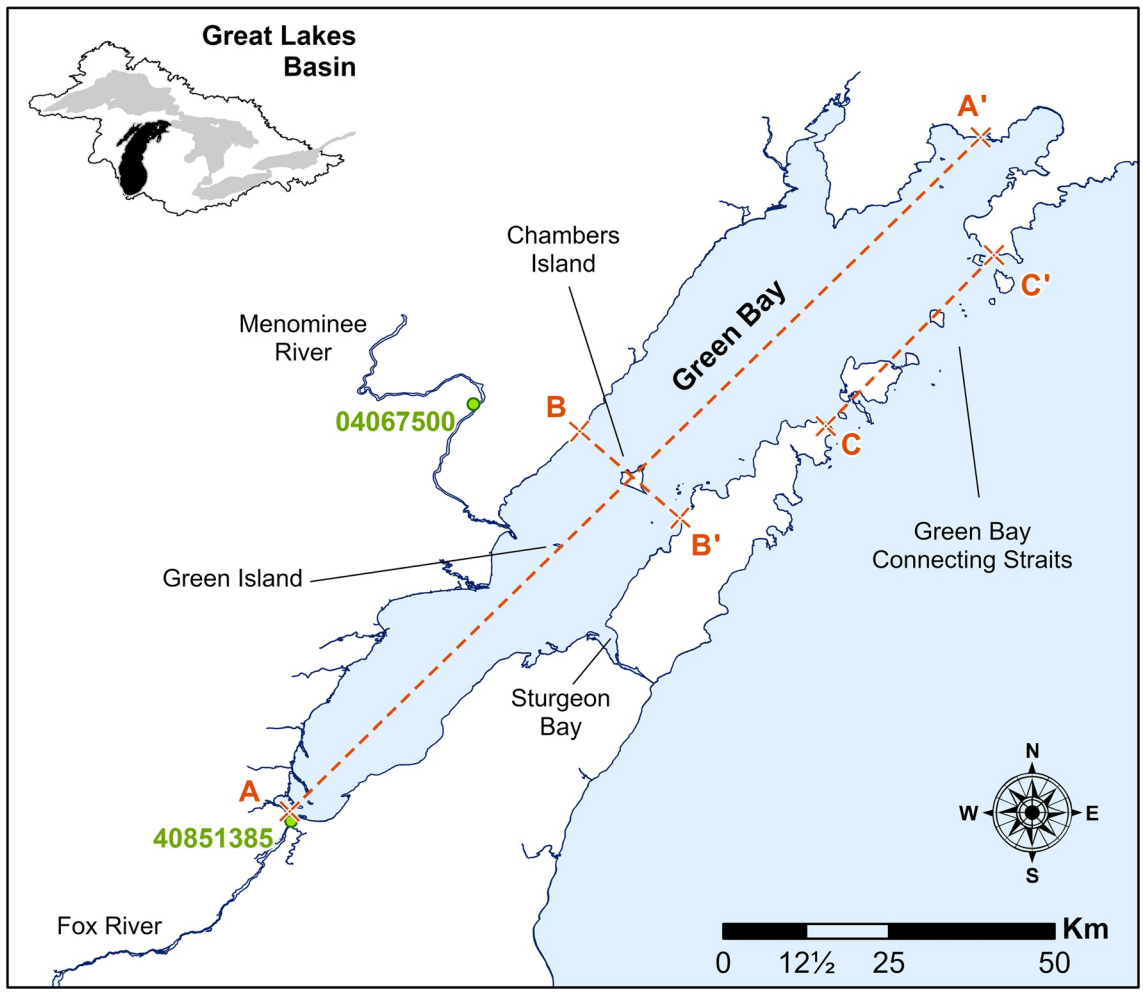

Station Name	Station ID	Lat	Lon
Southern Green Bay Buoy	45014	44.80	-87.76
Milwaukee Atwater 20m Buoy	45013	43.10	-87.85
Northern Michigan Buoy	45002	45.34	-86.41
Southern Michigan Buoy	45007	42.67	-87.03
Sleeping Bear Dunes Buoy	45183	44.98	-85.83
Green Bay West Buoy	GBW	44.58	-87.99
Green Bay East Buoy	GBE	44.55	-87.96
NEW Water Station 13	NW13	44.53	-88.01
USGS Fox River Gauge	40851385	44.53	-88.01
USGS Menominee River Gauge	04067500	45.33	-87.66
USGS Lake Michigan at Gary	04092788	41.65	-87.43
USGS Lake Michigan at Hyde Park	04092440	41.78	-87.57

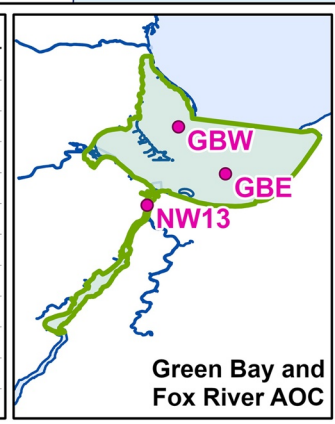

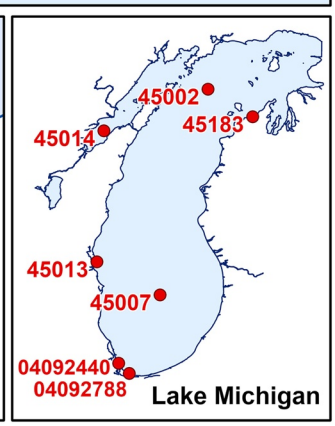

Figure 1. Green Bay Location in Lake Michigan and the Great Lakes basin. Lower insets show Lake Michigan and the Green Bay area of concern (AOC). Buoy stations and USGS gauges used in this study and their abbreviations are also shown in the Figure. Cross-sections A-A', B-B', and C-C' are used to look at transport patterns in different locations across the bay.

Martin, Poverty, Summer, and Little Summer Islands in the exchange zone of the Lake Michigan and Green Bay were incorporated in the grid (see Figure S2). Also, the coastline data was updated to include the Cat Island, a feature that is crucial in modeling the circulation and transport in the Green Bay AOC.

Bathymetry and shoreline data, used to generate the Lake Michigan unstructured grid (Figure S3), are based on NOAA datasets (National Geophysical Data Center, 2015; NOAA, 2017) and were updated in

Table 1
Sediment Properties and Erosion/Deposition Characteristics Used in the Lake Michigan Sediment Transport Model

Sediment class	1	2	3	4	5	6	Source
Sediment type	Clay	Fine Silt	Coarse Silt	Fine Sand	Coarse Sand	Gravel	Moore et al. (1973), Wisconsin DNR (2000), and Lee et al. (2007)
D_{50} (mm)	0.001	0.008	0.05	0.1	0.5	2	Jones (2000) and Yolcubal et al. (2004)
ρ_s (kg/m^3)	2,300	2,300	2,300	2,450	2,450	2,450	Wisconsin DNR (2000)
Φ (%)	97.5	97.5	97.5	85	75	60	Manchester-Neesvig et al. (1996)
ω (mm/s)	0.001	0.02	1.01	4.95	57.04	175.31	García (2008)
τ_{ce} (N/m^2)	0.008	0.029	0.09	0.18	0.25	1.10	García (2008)
E_0 (kg/m^2/s)	0.0005	0.0025	0.005	0.005	0.005	0.005	Ariathurai and Arulanandan (1978)

the southern Green Bay to represent recent changes of the bathymetry due to the dredging of navigational channel project.

The Lake Michigan grid in this study includes 52,574 triangular elements/cells, 28,985 nodes, and is vertically discretized to 20 σ-layers, that is, layers follow terrain variations that are uniformly distributed in the water column. The grid is designed very dense in Green Bay, where element side length varies between 50 to 1,500 m from the mouth of Fox River to upper Green Bay. Since the focus of our model is to simulate sediment transport in Green Bay, a coarser grid resolution is used for the main body of Lake Michigan for the sake of computational efficiency. Given the suggested summertime baroclinic Rossby radius of 5 km in the Great Lakes, it is critical to use a grid size less than 5 km within the 8–10 km of the coastal areas (Beletsky et al., 1997, 2006). Therefore, cell side length in the Lake Michigan grid was designed to vary between 1,000 m in the shorelines to about an average of 5 km in the central lake areas. A relatively fine grid is constructed near the connecting straits to be able to accurately account for the exchanges between the lake and the bay.

FVCOM-SWAVE offers various options suitable for the simulation of waves in different physical conditions (Booij et al., 1999, Table 1). In this study, the wave model was adjusted by selecting from those options based on recommendations in the literature (Mao et al., 2016; Ris et al., 1999), and our comparisons of simulated results against the validation buoys in nearshore and deep-water areas of Lake Michigan. In this regard, the third generation of the SWAN wave model (Booij et al., 1999) with quadruplet wave-wave interactions of Hasselmann et al.'s (1985) was adopted for this study. We also used Komen et al.'s (1984) formulation for wind growth and whitecapping, Hasselmann et al.'s (1973) expressions for bottom friction, and Battjes and Janssen's (1978) formulation for depth-induced breaking calculations. We also selected 60 as the number of steps in the relative frequency space.

3.3. Sediment Classification and Properties

Sediment transport models require a set of standard parameters for model simulations, which can be obtained through observations, lab experiments, and/or calibration. Those important parameters include particle density (ρ_s), mean diameter (D_{50}), and porosity (φ). Prediction of sediment transport is also very sensitive to erosion and deposition characteristics of the particles such as critical shear stress for erosion (τ_{ce}) and settling rates (ω). A previous Lake Michigan sediment transport model has found ~40% deviations in results by changing these parameters (Lee et al., 2005), yet, the model had the most sensitivity to the fraction of fine-grained particles in the sediment mixture. Therefore, it is important in the first place to define the distribution of sediment classes in the bed layer.

We extracted information from several studies to obtain a general understanding and reasonable estimates of sediment characteristics in Green Bay. The next steps included using soil classification methods/standards

and consultation with experts to narrow down the ranges defined for each parameter in the literature. Finally, some of these model parameters were adjusted based on model calibration.

There are few studies of Green Bay sediment classes and their distribution. Field observations and analysis of sediment samples (HydroQual Inc., 1999; Jones, 2000; Moore et al., 1973; Wisconsin DNR, 2000) have found clay, silt, and sand are the major constituting variables of lower Green Bay. As we move from south, near the mouth of Fox River, to the north, near the connecting straits, mud content decreases in the bed layer and the upper Green Bay bed is mostly formed by sand and gravel. We compiled these findings with Lee et al.'s (2007) recommendations for Lake Michigan and estimated bottom sediment stratigraphy as shown in Figure S4. These patterns are also consistent with distributions of cohesive sediment in Green Bay (HydroQual Inc., 1999). It is important to mention that the composition of the benthic zone in Lake Michigan has changed due to the invasion of Zebra and Quagga Mussels. Zebra mussels were first observed in Green Bay in 1991 and Quaggas in 2003. In lower Green Bay and the inner bay, the distribution of dreissenid mussels is patchy (Qualls et al., 2013) and in the depositional areas of the bay they are absent. This is almost certainly due to recurring summertime hypoxia in the mid and lower bay (Kaster et al., 2018; Klump et al., 2018). Hypoxic events have also been repeatedly observed from time series dissolved oxygen sensors deployed recently in the shallow waters of the inner bay. The influence of dreissenid on sediment resuspension is difficult to judge with certainty, but would appear minor relative to physical processes. Those changes are neglected in the assignment of bottom sediment initial conditions, yet have to be considered in future studies for improved simulations of sediment transport when sufficient information becomes available (see Figure S5).

We identified six sediment classes for the current model development and determined sediment mean diameter based on the U.S. Department of Agriculture (USDA) soil classification standard (Yolcubal et al., 2004) as shown in Table 1. Density and porosity of different sediment classes were also estimated based on the analysis of sediment samples taken in Green Bay (Manchester-Neesvig et al., 1996; Wisconsin DNR, 2000).

Previous studies have shown wide ranges of sediment settling/fall velocity in Green Bay. NOAA sediment trap study found settling velocities of about 6–70 mm/s in stratified conditions (summertime) and 14–200 mm/s during unstratified periods. We used a method proposed by Soulsby (1998) that estimates fall velocity based on sediment mean diameter and density and viscosity of water. This method is suitable for fine-grained sediments, therefore, we used for coarser sediment classes a graphical method explained by García (2008, p. 42), which requires the same variables as Soulsby's method.

While settling velocity governs deposition, bottom erosion and resuspension events are controlled by critical shear stress for erosion which we estimated based on the definition of Shields nondimensional critical shear stress (τ_c*). τ_c* can be found based on the modified Shields diagram (Parker, 2004) or alternatively for finer particles based on Mantz's (1977) empirical relationship. Critical shear stress for erosion is then a function of τ_c*, particle density, and mean sediment diameter according to the Shields formulation.

FVCOM-SED requires a bed erodibility constant (E_0) in order to estimate bottom sediment fluxes. A wide range of values is suggested in the literature for E_0. Ariathurai and Arulanandan (1978) conducted several tests on more than 200 natural or lab-synthesized fine and cohesive sediment samples and suggested values between 5×10^{-4} and 5×10^{-3} kg/m^2/s. Analysis of those samples has shown that the slope of erosion rate curves increases proportionally to critical shear stress for erosion.

3.4. River Inputs

Tributary loadings are the major input fluxes into Green Bay. Required river inputs for the circulation, wave, and sediment transport models are discharge, temperature, and total suspended solids (TSS) at river mouth that were estimated in this study based on daily USGS observational data. USGS observations during the 2011–2019 period show average inflowing discharge of 170, 24, 29, and 106 m^3/s and TSS concentrations of 24, 0.24, 0.03, and 3 mg/L for the Fox, Oconto, Peshtigo, and Menominee Rivers, respectively. Those statistics indicate that the Fox and Menominee Rivers have more influence on circulation and thermal regimes in Green Bay, hence they were included as boundary conditions of the model.

It should be noted that riverine TSS loading into the bay is estimated based on empirical relationships developed using USGS observations of discharge and turbidity at the mouth of Fox River (gage ID: 40851385)

and cruise measurements of turbidity and TSS by the city of Green Bay Sewerage district, now NEW Water, at this location (Khazaei, 2020; Khazaei et al., 2018; NEW Water, 2017). The Fox River sediment load composition varies by flowrate. For the regular summertime flowrates in the Fox River (less than ~300 m^3/s), observations by Jones (2000) show that ~50% of Fox River sediments are very fine materials with mean diameter size less than 0.005 mm, ~40% are materials with a mean dimeter of 0.05 mm, and ~10% are coarser materials. Therefore, we assumed 50% Clay, 35% Fine Silt, 10% Coarse Silt, 3% Fine Sand, and 2% Coarse Sand in the incoming river loads.

3.5. Field Data and External Forcing

Previous efforts in modeling physical and biogeochemical processes in Green Bay have been challenged by the scarcity of relevant hydrodynamic and water quality observational data. Recent data collection efforts, such as continuous monitoring of turbidity at Green Bay West and East buoys in the southern bay (Miller, 2020), have made the development and validation of a sediment transport model for Green Bay possible. As explained above, we used NEW Water turbidity and TSS cruise data to convert turbidity observations into TSS time series. In addition, seven buoy stations in Lake Michigan and Green Bay were used to validate hydrodynamic and wave models, that is, southern Green Bay, Atwater Beach in Milwaukee nearshore zone, Sleeping Bear Dunes, North Michigan, and South Michigan buoys (see Figure 1).

External forcing inputs used in the model includes 2 m air temperature, surface air pressure, 10 m wind, dew point temperature, and cloud cover and are based on the interpolation of NOAA National Centers for Environmental Information (NCEI; NOAA, 2018) land-based and buoy stations in the Great Lakes basin. The interpolation scheme is based on a natural neighbor method developed by NOAA Great Lakes Environmental Research Laboratory (GLERL) for application in the Great Lakes forecasting models (Beletsky et al., 2003; Schwab & Beletsky, 1998) and accounts for adjustments of overland to overlake conditions whenever data from land-based stations were used (Beletsky & Schwab, 2001). This method has been employed in NOAA operations since 2005 for the Great Lakes with favorable results for water temperature, waves, circulation, and other hydrodynamic variables (Rowe et al., 2015). The surface heat fluxes are calculated using the FVCOM SOLAR option in the model, which is an approach prescribed based on bulk transfer equations (Cotton, 1979; Guttman & Matthews, 1979; Ivanoff, 1977; Wyrtki, 1965; Xue et al., 2015) and developed for the Great Lakes Coastal Forecasting System (GLCFS) by NOAA/GLERL (NOAA, 2021b).

3.6. Model Skill Criteria

We use Root Mean Squared Error (RMSE), Bias Deviation (BD), and correlation coefficients (CC) to assess model skills of scalar variables (e.g., temperature and TSS):

$$\mathrm{RMSE} = \frac{1}{N}\left(\sum_{i=1}^{N}\left(e_i^2\right)\right)^{1/2} \tag{8}$$

$$\mathrm{BD} = \frac{1}{N}\sum_{i=1}^{N}\left(e_i\right) \tag{9}$$

$$\mathrm{CC} = \frac{\sum_{i=1}^{N}\left(x_{i,O} - x_{\mathrm{ave},O}\right)\left(x_{i,P} - x_{\mathrm{ave},P}\right)}{\left[\sum_{i=1}^{N}\left(x_{i,O} - x_{\mathrm{ave},O}\right)^2\right]^{1/2}\left[\sum_{i=1}^{N}\left(x_{i,P} - x_{\mathrm{ave},P}\right)^2\right]^{1/2}} \tag{10}$$

where N is the number of observation/prediction points, e_i is the deviation of the predictions from observations (i.e., $e_i = x_{i,O} - x_{i,P}$; where $x_{i,O}$ and $x_{i,P}$ are observational and prediction values at point i, respectively), and $x_{\mathrm{ave},o}$ and $x_{\mathrm{ave},P}$ are the mean of observed and predicted data, respectively.

To assess model skills for vector fields (e.g., currents) we use normalized Fourier norm (F_n) and average angular difference ($\Delta\theta$):

$$F_n = \frac{\| V_o, V_p \|}{\| V_0, 0 \|} = \frac{\left(\frac{1}{N} \sum_{i=1}^{N} \left| V_{i,o} - V_{i,p} \right|^2 \right)^{1/2}}{\left(\frac{1}{N} \sum_{i=1}^{N} \left| V_{i,o} - 0 \right|^2 \right)^{1/2}} \quad (11)$$

$$\Delta\theta = \frac{1}{\pi N} \sum_{i=1}^{N} \cos^{-1} \left(\frac{V_o . V_p}{|V_o||V_p|} \right) \quad (12)$$

where $V_{i,o}$ and $V_{i,p}$ denote observed and predicted vector fields at point i, respectively.

RMSE is used to assess model accuracy, that is, zero indicates perfect model accuracy and as the value increases, model accuracy decreases. BD shows model bias and smaller values close to zero denote lower biased performance of the model. CC can be used as an indicator of model performance in reproducing the temporal patterns of change in observational data. In this article, CC is reported if significant at p-value ≤0.05. Fn and $\Delta\theta$ assess model accuracy in the prediction of vector fields magnitude and direction, respectively. F_n and $\Delta\theta$ equal to zero indicate a perfect model, values between zero and one are in the acceptable range, and as the value increases, model performance decreases.

4. Simulation Details and Model Validation

We ran the model for the 2016–2019 years and model simulations were limited to the May-October period of each year to focus on the ice-free period in Lake Michigan and time of active bottom layer sediment dynamics. Model stability requires simulations at a time step of 5 s. The circulation model is initiated at rest, that is, zero currents. 3D temperature fields are interpolated from LMHOFS simulation in Lake Michigan at the initial condition. LMHOFS uses FVCOM as its core circulation model and provides high-resolution forecasts of water level, currents, and water temperature for Lake Michigan and Huron system which we used for the interpolation of temperature fields (NOAA, 2021a). Also, the model is run using realistic initial water surface elevation in Lake Michigan (NOAA, 2020). We ignored major open boundary conditions around Lake Michigan, for example, bi-directional flow at the Straits of Mackinac and Chicago River diversion, because they do not have an immediate impact on sediment transport in Green Bay, especially southern areas in the bay.

The bed layer and bottom sediment distribution are initialized in each year based on the non-uniform distribution of different sediment classes defined in Section 3.3 (see Figure S4). Considering the average bottom distribution over the entire lake, the portion of cohesive (Clay, Fine Silt, and Coarse Silt) and non-cohesive (Fine Sand, Coarse Sand, and Gravel) sediment classes contributing to the bottom layer are 29% and 71%, respectively, that is, cohesive sediments are defined as the mixture of clay and silt (Wolanski, 2007). Analysis of sediment samples in Green Bay showed that the average cohesive sediment depth in Green Bay is ~0.5 m (Wisconsin DNR, 2000). Average erosion and deposition patterns in Green Bay, as well as Lake Michigan (Lou et al., 2000), showed that bed changes do not exceed that value during long-term simulations of semi-annual to annual scales. Therefore, we started the model with a bed thickness of 0.5 m. We also conducted a sensitivity analysis of TSS simulations at GBE and GBW and found that although results are slightly sensitive to initial bed thickness, values in the range 0.25 and 0.5 m result in a reasonable estimation of TSS simulations in Green Bay.

4.1. Validation of Simulated Currents, Waves, and Temperature Fields

Currents are the main driver of transport mechanisms in hydrodynamic simulations. Accurate simulations of sediment transport dynamics rely on accurate simulations of currents near the bottom. Figure 2 compares the observed and predicted daily currents in N-S (v component) and E-W (u component) directions during the May–October of 2016–2019 years. Comparison plots and model skill criteria indicate reasonable agreement between model and buoy observations at two selected locations, given the complex nature of the physical process and the system. Our calculated model skill statistics for currents (or velocity fields) are comparable and in some cases show slight improvements compared with previous Lake Michigan

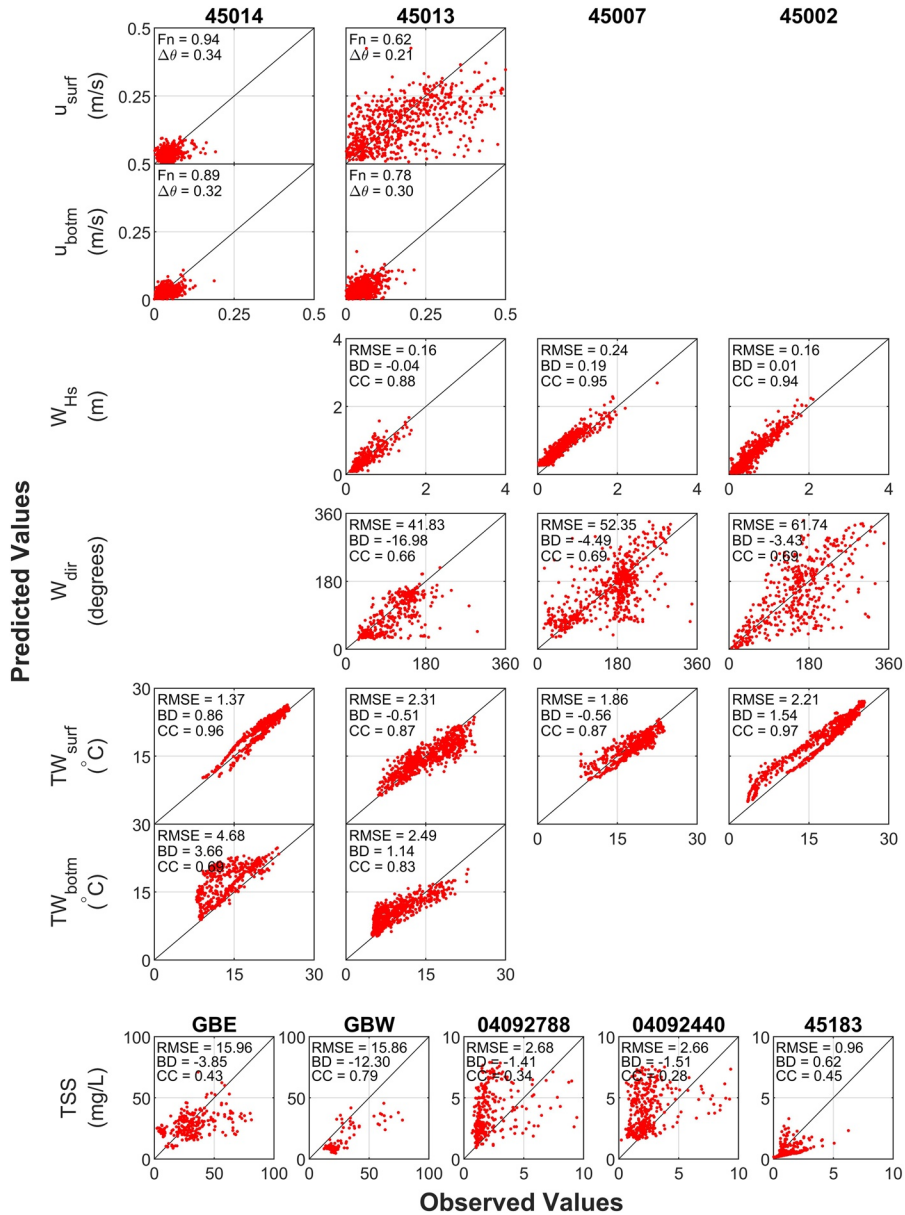

Figure 2. Comparison of the daily observed and predicted surface and bottom currents (u_{surf} and u_{botm}), significant wave height (W_{Hs}) and direction (W_{dir}), surface and bottom temperature (TW_{surf} and TW_{botm}), and total suspended solids (TSS) at the location of selected validation buoys during 2016–2019 years. Buoy locations are shown in Figure 1. CCs are reported if significant at P-value ≤0.05.

hydrodynamic modeling efforts. For example, *Fn* values of 0.79–1.01 and 0.9–1.05 were reported respectively for barotropic (Schwab, 1983) and POM-based (Beletsky & Schwab, 2001) models of summertime circulation in Lake Michigan built on 5-km resolution grids. Rowe et al. (2015) obtained improved performance in modeling summertime hydrodynamics by using interpolated forcing and adopting FVCOM, and reported *Fn* values of 0.83–0.91. Schwab (1983) and Rowe et al. (2015) have respectively reported values of 0.23–0.46 and 0.29–0.31 for $\Delta\theta$ in modeling Lake Michigan currents direction. Wave action complements currents to force sediment movement. Combined current-wave action produces stronger shear stresses at the water-sediment interface and triggers more frequent and/or stronger episodes of resuspension. Hence, an accurate wave model will improve the understanding of sediment processes.

Figure 2 shows the comparison of observed and predicted significant wave heights (W_{Hs}) and wave directions (W_{dir}). W_{Hs} is defined as the average of the highest one-third of the waves, measured between wave trough to crest. According to the figure and model skill statistics, FVCOM-SWAVE simulations of wave height are in good agreement with observations at three selected buoys. In particular, high correlations between observations and simulations implies that patterns of the wave height variability are reproduced well by the model. However, wave direction predictions are not as accurate as wave heights. Comparison of the model skill statistics with previous wave models of Lake Michigan (Hawley et al., 2004; Mao et al., 2016) also suggests a good (in some cases improved) performance by the FVCOM-SWAVE model and its suitability for applications in modeling sediment transport.

We also validate predictions of temperature fields to assess the performance of the physical model in simulating circulation and transport. Also, temperature governs biogeochemical processes in the lake and is important for Green Bay restoration studies. As shown in Figure 2, the temperature is predicted with high accuracy at four selected buoys, except for over-estimation of mid-range bottom temperature at the location of Green Bay buoy station 45014. One possible explanation for that is the model's inability to fully capture cold water intrusion from Lake Michigan into the southern bay. Denser cold water from the lake flows near the bottom while warmer water, coming into the bay from rivers, flows on top; forming a two-layered flow condition in Green Bay (Grunert et al., 2018). Yet, high correlations between predicted and observed water temperature at this location, as well as other buoys, shows that the model is capable of producing the patterns of variability in temperature profiles such as upwelling events.

4.2. Validation of Simulated Total Suspended Solids

Figure 2 compares predicted daily TSS against the observations at five different locations in Green Bay and Lake Michigan, where turbidity observations are available in 2016–2019. Turbidity times series obtained at those locations were converted into TSS concentration using TSS-turbidity empirical functions for the estimation of river loadings (explained in Section 3.4). GBW and GBE buoys are located in very shallow areas of lower Green Bay (~1 m depth) and sensor probes were placed at the middepth water column; therefore, observations represent the bottom sediment conditions. USGS 04092788 and 04092440 buoys are located in southern and southwestern Lake Michigan where multiple episodes of sediment resuspension events occur during the May–October period. Great Lakes Observing System (GLOS) 45183 buoy is located at Sleeping Bear Dunes in northeastern Lake Michigan with complex geomorphological characteristics of the lake that complicates sediment dynamics. 04092788, 04092440, and 45183 buoy stations represent surface conditions.

Figure 2 implies a fairly good accuracy and overall satisfactory performance of the model in modeling sediment transport in Green Bay AOC, given the physical complexity of the system. Although the model is biased at GBW buoy, high correlations between observed and predicted TSS values at GBW denotes model capability in the simulation of storm events and episodes of resuspensions. Figure S6 illustrates examples of resuspension events captured by the model at these two locations. In some cases, the model significantly underestimated TSS observations at both buoys. Those underestimations may be explained by sensor malfunction and/or sudden spikes of TSS concentrations due to construction activities near the GBW buoy (e.g., Cat Island project), dredging of Fox River, and navigation channel project.

Although the sediment model is focused on Green Bay, TSS validations at southern Lake Michigan (04092788 and 04092440 buoys) and Sleeping Bear Dunes (45183 buoy) are fairly satisfactory (Figure 2). Figure S6 also shows that the model is able to produce the patterns of high-turbidity episodes in these distinct locations in southern and northern basins of Lake Michigan, although the magnitude of high resuspension events is not completely accurate.

In addition to those validations based on buoy data, we compared model results with direct measurements of TSS made by NEW Water at four stations in lower Green Bay (Figure 3a). NEW Water collects samples at those locations during summertime and provides middepth observations of TSS by lab analysis of the collected samples. Given that there is high variability in sediment dynamics in the shallow waters of lower Green Bay, where NEW Water makes these measurements, the model shows a fairly good performance in predicting the sediment fields in this area.

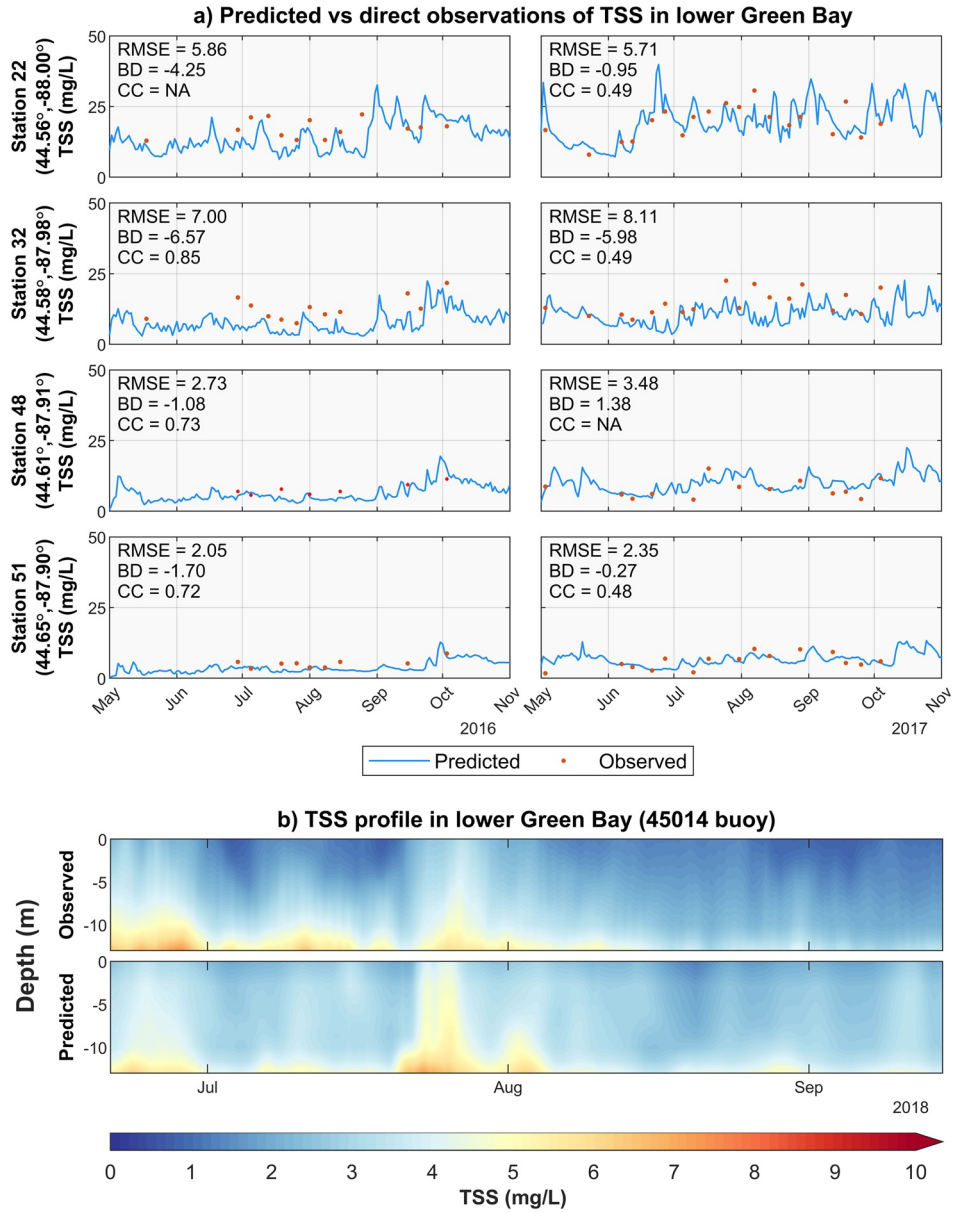

Figure 3. (a) Comparison of the middepth observed and predicted total suspended solids (TSS) in lower Green Bay at NEW Water stations 22, 32, 48, and 51 that are located 2.23, 5.16, 11.88, and 15.23 km from the mouth of Fox River and are approximately 8, 8.5, 6, and 9 m deep, respectively, and (b) comparison of the observed and predicted TSS profiles in lower Green Bay (45014 buoy) in 2018.

NEW Water samples showed that high concentrations of Chlorophyll-a (*Chl-a*) occurred from late June until mid-September, 2016 at stations 22 and 32. Similar concentration pattern was observed at those two locations from mid-July until late August, 2017. Our model results showed more deviations from observations during those 2016 and 2017 periods, probably due to the presence of organic suspended materials. There were smaller differences between observed and predicted TSS values at stations 48 and 51 (in a further distance from the mouth of Fox River) where *Chl-a* concentrations are smaller.

We also compared observed and predicted TSS profiles in lower Green Bay (45014 buoy) in 2018 to assess model skills in the simulation of vertical sediment profiles (Figure 3b). Observational TSS profiles were inferred from the acoustic backscattering signal collected by *Nortek Aquadopp 600 kHz* Acoustic Doppler current profilers (ADCP) at 10 depth layers (GLOS, 2021). Backscattering signal was converted from echo

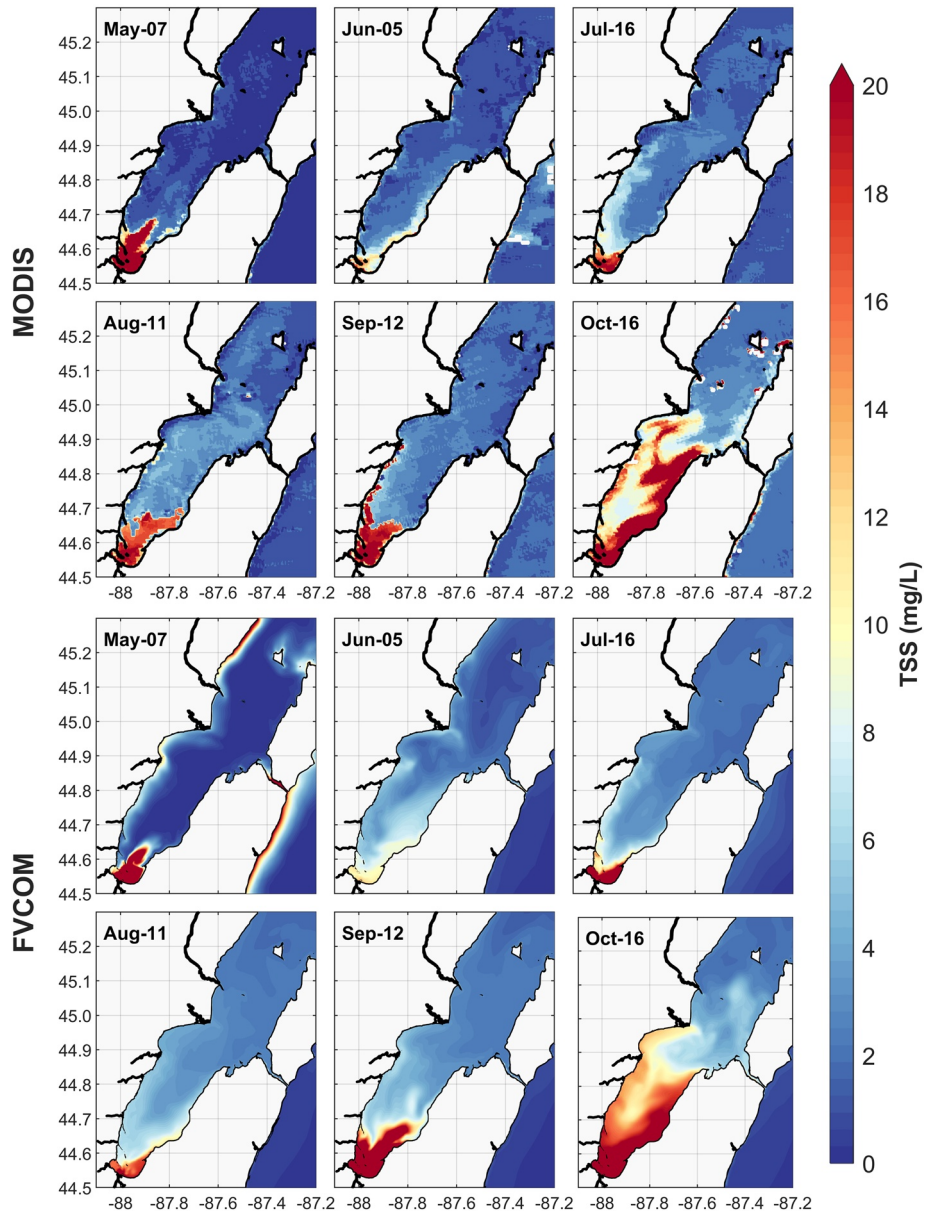

Figure 4. Snapshots of the surface total suspended solids (TSS) in Green Bay for six cloud-free selected days in May–October 2018 period based on MODIS imagery (top) and FVCOM simulations (bottom).

intensity based on a procedure explained and used in previous studies (Deines, 1999; Lee et al., 2007). The backscattering signal was paired with turbidity data from a deployment at the Green Bay buoy station 45014 in July 2016. Turbidity data were collected by a *WET Labs NTUSB* turbidity sensor and were used to build relationships between turbidity and ADCP backscattering signal. Those relationships are used to estimate turbidity profiles, which were converted to TSS concentration profiles based on the empirical TSS-turbidity functions explained in Section 3.4.

Figure 3b shows that the predicted TSS profiles are similar to the patterns of the observed profiles and indicate the simultaneous occurrence of high-turbidity events, although the magnitude of TSS concentration deviates slightly during storm events. Comparison of the depth-averaged observed and predicted TSS profiles results in RMSE, BD, and CC skill metrics of 1.31 mg/L, −0.83 mg/L, and 0.47 at the Green Bay buoy station 45014. These model performance metrics show that the model is skillful in the simulation of TSS over the water column.

Besides these point validations of the model's ability to predict TSS, we conducted a spatial validation of model skills in simulating TSS using satellite data. Figure 4 compares the surface snapshots of TSS concentration based on FVCOM simulations and MODIS imagery for six selected days in 2018. MODIS-based TSS maps are estimated based on a procedure explained in Hamidi et al. (2017), using relationships developed between simultaneous surface reflectance and NEW Water TSS observations at the location of monitoring stations in lower Green Bay. We used MODIS product *MYD09GA* for the estimation of surface TSS. We picked several days during the summer of 2018 by visual inspection, and then used *MYD09GA Surface Reflectance 500 m Quality Assurance* and *1 km Reflectance Data State QA* layers to filter high-quality and cloud-free data. True-color visualization of raw imagery data is presented in Figure S7. Except for small deviations in August that could be explained by inaccurate estimation of TSS inputs and/or wind conditions, the model-simulated spatiotemporal patterns of TSS in lower Green Bay and decreasing gradient of suspended particles from Green Bay AOC toward Chambers Island match very well with the results of the remote sensing method.

The array of validation methods used, including point validations of predicted TSS concentration, assessment of model performance during the high-turbidity events, validation of model's capability in reproducing the TSS profiles, and spatial comparison of the surface TSS patterns with satellite imagery data indicate a reasonable accuracy of the physical sediment transport model. During summertime when bloom events can cause high-turbidity events, the physical TSS model can be improved by coupling it with a biogeochemical model. As we will discuss with more details in the next sections, our results also agree with the findings of previous studies and qualitatively matches the patterns of the bottom shear stress forces and sediment transport in Lake Michigan (Lee et al., 2005, 2007; Lou et al., 2000).

5. Results and Discussion: Summer Circulation and Transport Regimes in Lake Michigan and Green Bay

The summer circulation and transport regimes are analyzed in Sections 5.1–5.4 in terms of monthly average fields of wind-induced currents and waves action, bottom shear stress driven by waves and currents, thermal structure, and sediment transport. The results of this study are shown to complement previous modeling studies of Lake Michigan and to provide important additional details on the circulation and transport regimes in Green Bay. Section 5.5 presents and analyzes a climatological study of the summer circulation and transport regimes in Lake Michigan. Section 5.6 summarizes previous studies on lake sediment dynamics, biogeochemical interactions, HABs, and the role of mussels, and considers the potential application of the approach developed in this study to investigate those processes.

5.1. Monthly Averaged Wind-Induced Circulation and Wave Action

Circulation and wave actions in Lake Michigan are predominantly wind-driven (Beletsky et al., 2006), and wind affects the exchange between Green Bay and Lake Michigan (Waples & Klump, 2002). Figure 5 shows monthly averaged wind patterns over Lake Michigan, with higher resolution over Green Bay, during the 2016–2019 simulation period, where dominant wind patterns are estimated using *streamline* function in MATLAB and highlighted in red colors. The figure shows stronger wind fields in northern Lake Michigan, as southerly winds accelerate over the approximately 500 km lake's longitudinal fetch. Winds are stronger in July–October with prevailing southwesterly and southerly general regimes. Wind patterns over Green Bay are more uniform, yet consistent with winds over Lake Michigan. Eastern winds dominate in May–June, and the wind fields shift to southwesterly and southerly directions in July until October, when winds are the strongest. Analyses of wind fields in the Great Lakes basin, including Lake Michigan, have shown prevailing southwesterly winds during summer, with monthly and seasonal shifts in wind direction/magnitude during 1980–1999 (Waples & Klump, 2002) and Green Bay during 2004–2008 (Hamidi et al., 2015).

In consistency with previous analyses of monthly averaged circulation in Lake Michigan (Beletsky et al., 2006), Figure 6 shows that cyclonic (counterclockwise) circulation dominates Lake Michigan. Also, currents drive gyres in the lake, and the formation of gyres is more common in the southern basin. Strong currents at the exchange zone affect water, heat, and sediment fluxes between Lake Michigan and Green Bay. In consistency with wind patterns, circulation is weaker in May and currents accelerate starting in June.

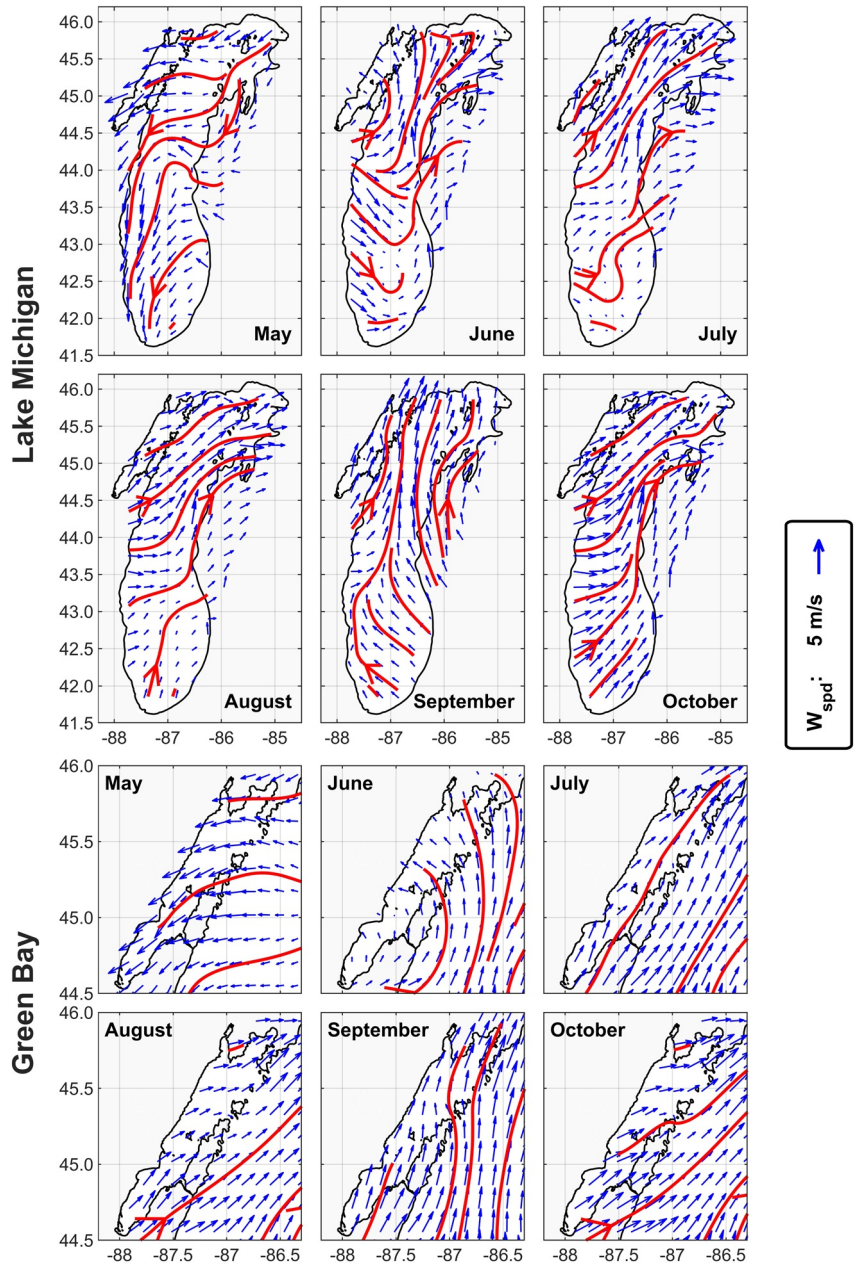

Figure 5. Monthly averaged wind patterns over the surface of Lake Michigan and Green Bay during the period of 2016–2019 years. Bolded red lines indicate dominant wind patterns. W_{spd} denotes wind speed.

Bimonthly analysis of currents in the May–October period in Lake Michigan in 1982–1983 and 1994–1995 also suggests that currents magnitude increase from May to October and currents move counterclockwise and are stronger in the nearshore areas of the southern basin of the lake. Similar to wind fields, dominant current patterns are estimated using *streamline* function in MATLAB and highlighted in red colors.

In Green Bay, the currents show more spatial variability than the wind fields, with the widespread formation of gyres, particularly north of Chambers Island and near the exchange zone with Lake Michigan, where strong currents are observed. Currents are generally in the north direction and stronger near the western shore of the bay. Most of these patterns, in particular stronger nearshore currents and frequent formation of gyres in Green Bay during summer, have shown by previous efforts in the simulation of currents in Green

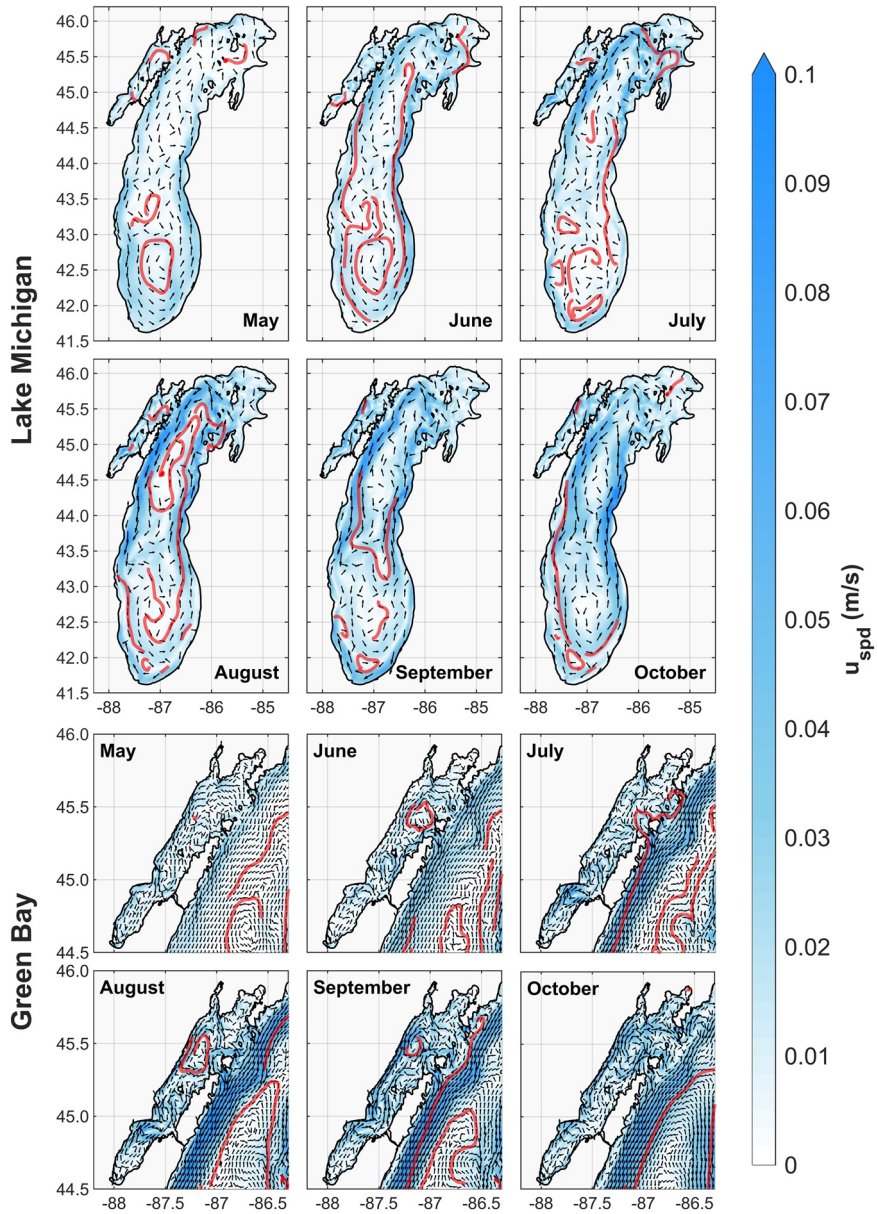

Figure 6. Monthly and depth-averaged currents in Lake Michigan and Green Bay during the period of 2016–2019 years. Bolded red lines indicate dominant circulation patterns. u_{spd} denotes currents magnitude.

Bay for the 2004–2008 period using a POM-based circulation model (Hamidi et al., 2015). Those patterns are present along the water column, although currents are much stronger in the surface (Figures S8 and S9).

Current movement and transport in Green Bay are significantly restricted by morphology and lake bottom terrain. Figure 7 shows monthly averaged horizontal current profiles, based on 2016–2019 simulations, along the three cross-sections shown in Figure 1. As illustrated in cross-section A-A' (where red colors show northward currents and blue colors show southward currents along the section), the currents in southern Green Bay (i.e., south of Chambers Island, located at 85 km)—which play a main role in the transport of Fox River loads to the northern bay—shift direction in June and move toward the south in the longitudinal cross-section A-A'. The southward current pattern is driven by a combination of wind direction and cold-water intrusion from the lake into the bay as mentioned above. Current profiles north of Chambers Island and south of the exchange zone (between 85 and 130 km) are different from the rest of the cross-section. Those patterns can be explained by the presence of gyres in that area, especially away from the shorelines and in

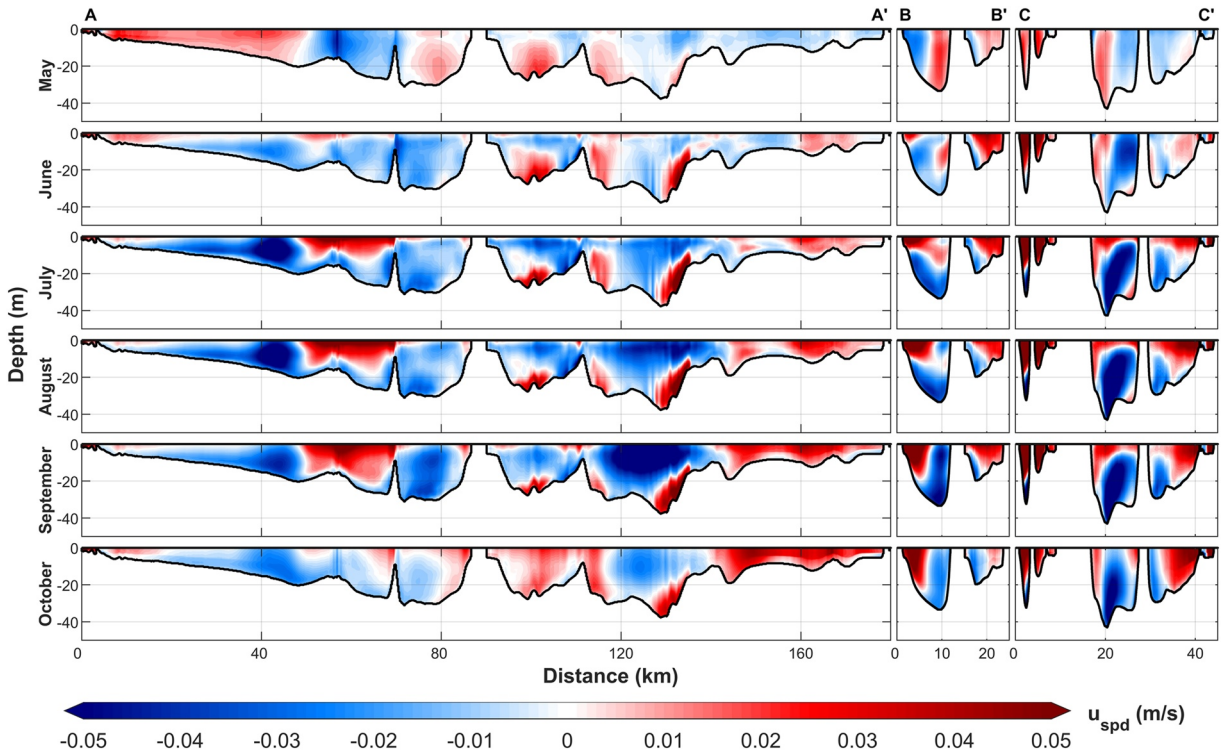

Figure 7. Monthly averaged current profiles along the A-A' (Green Bay longitudinal axis), B-B' (Chambers Island), and C-C' (connecting straits) cross-sections (as shown in Figure 1) during the period of 2016–2019 years. The vertical axis is exaggerated ~700 times. u_{spd} denotes currents magnitude. Colors show current directions along the A-A' cross-section (red/blue indicates northward/southward) and perpendicular to B-B' and C-C' cross-sections (red/blue indicates into/out of cross-sections, respectively).

the central bay areas where cross-section A-A' cuts through. Figures S8 and S9 show clearly that the surface currents in Green Bay are predominantly flowing north (especially near the shorelines) and bottom currents flow toward the south, providing more evidence for the summertime stratified flow conditions in the bay.

The current patterns in cross-section B-B' (where red colors show northward currents and blue colors show southward currents perpendicular to the section) show that currents in the western side of Chambers Island are strong and predominantly toward the south. The prevailing southward and northward currents through the western and eastern sides of Chambers Island, respectively, imply a counterclockwise circulation around the island, as shown in previous studies based on field observations (Hawley & Niester, 1993). Cross-section B-B' shows that, while surface currents are conveying water north, strong currents are moving toward the south near the bottom. Current profiles at cross-section C-C' (where blue colors show currents flowing into the bay and red colors show currents flowing out perpendicular to the section) also provide evidence that lake cold-water intrusion into the bay occurs persistently through deeper sections of the exchange zone profile. Similar to conditions in Chambers Island, currents are regularly swirling around the small islands in this area.

Currents are the dominant driver of circulation and heat transfer in lake systems, yet waves contribute significantly to sediment dynamics, through bottom interactions and resuspension events. According to Figure 8, wave action in Lake Michigan is limited in May–August, gradually increases in September, and escalates in October. In general, the northern basin of Lake Michigan experiences stronger waves, most probably due to dominant southern winds during the modeling period. The wind-dependency of wave actions in Lake Michigan was shown by previous modeling storm and surge peak events (Mao et al., 2016; Mao & Xia, 2017).

In concert with Lake Michigan, waves in the bay are stronger in September and October. Upper Green Bay and the exchange zone experience stronger waves probably due to rapid change in the bottom elevation in that area. As the incoming waves, originated in deep central areas of Lake Michigan, approach shallow

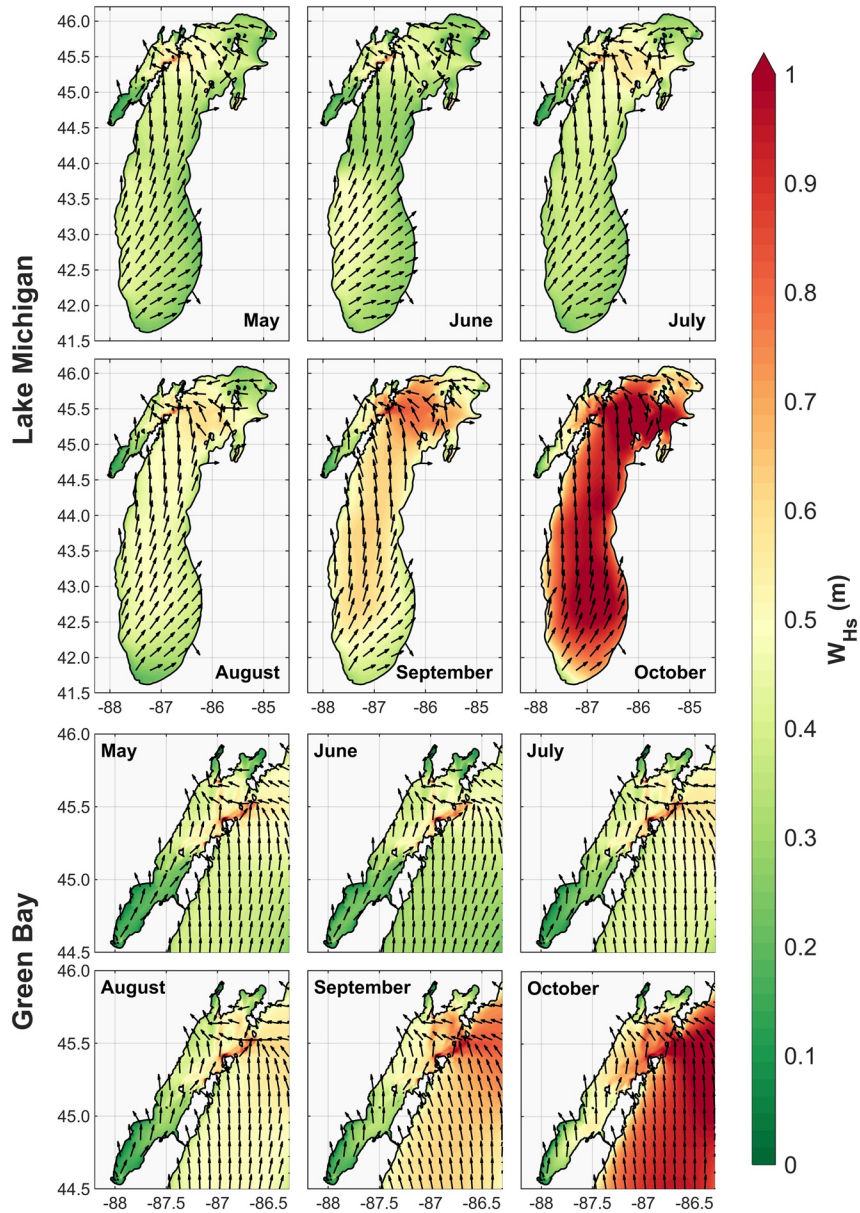

Figure 8. Monthly averaged significant wave height (W_{Hs}) in Lake Michigan and Green Bay during the period of 2016–2019 years.

waters of Green Bay and small islands at the connecting straits, water depth quickly starts to become less than the wavelength, reducing wave propagation velocity and leading to steepening of the waves and increased wave height.

5.2. Current-Wave Induced Bottom Shear Stress

Bottom shear stress governs resuspension events and sediment availability in the water column. Figure 9 shows the calculated monthly averaged bottom shear stress due to the combined effects of current-wave action. While higher shear stress near coastal areas is associated with the stronger nearshore currents, increased wave action in September and October results in augmented shear stress during those months. Western coastal regions, southern and northern shallow areas, and the connecting straits experience higher stress in Green Bay. Also, one would expect strong and frequent resuspension to occur in lower Green Bay

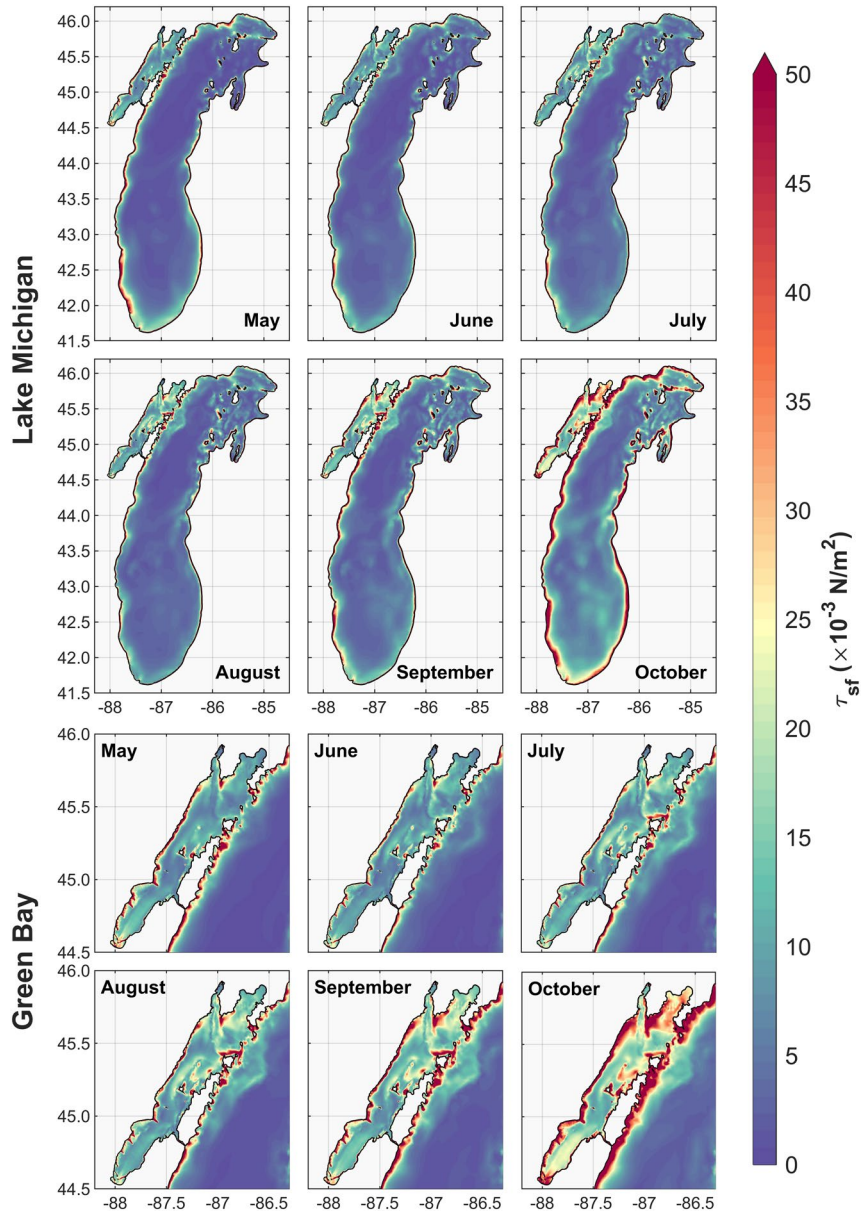

Figure 9. Monthly averaged bottom shear stress (τ_{sf}) due to combined effects of currents and waves in Lake Michigan and Green Bay during the period of 2016–2019 years.

in October, produced by the bottom shear stress forcing patterns during that month. Increased shear stress in southwestern Lake Michigan during May is probably associated with a lake-wide cyclonic gyre in the southern basin driven by widespread and strong northerly winds in that area. Southwestern coastal areas of Lake Michigan do not experience such strong wind regimes again until October. Those patterns, in particular high shear stress in the southern and western nearshore areas of Lake Michigan and southern, western, and northern Green Bay, compare well with current and wave bed shear distribution during a March 1998 episode shown by Lee et al. (2007), as well as average shear stress patterns in Lake Michigan during 1994–1995 (Lou et al., 2000).

To investigate the distinct contribution of waves and currents in driving physical forces in the lake, we simulated bottom shear stress without waves (currents only) and compared the results with the combined current-wave conditions. As expected, results indicated that for the May-October period of 2016–2019 years, on average the bottom shear stresses were higher by 494%, 334%, and 296% in Lake Michigan, Green Bay,

and lower Green Bay, respectively, when combined physical processes are considered, compared to the case when only currents are driving bottom shear stresses. Figure S10 and Table S1 compare the average spatial patterns of bottom shear stress in Lake Michigan and Green Bay under the two different physical forcing scenarios for the simulation period of 2016–2019 years. We expect to observe similar impact on TSS patterns in the lake due to these different driving stress scenarios. It is obvious that current-wave-induced forces play an important role in sediment plume development and transport. As shown in previous studies, the effects of waves are significant in shallow nearshore waters of Lake Michigan and Green Bay (Lou et al., 2000).

5.3. Thermal Structure of the System

Lake Michigan May–October monthly averages surface temperature fields are illustrated in Figure 10, based on 2016–2019 simulations. The southern basin of Lake Michigan is generally warmer than the rest of the

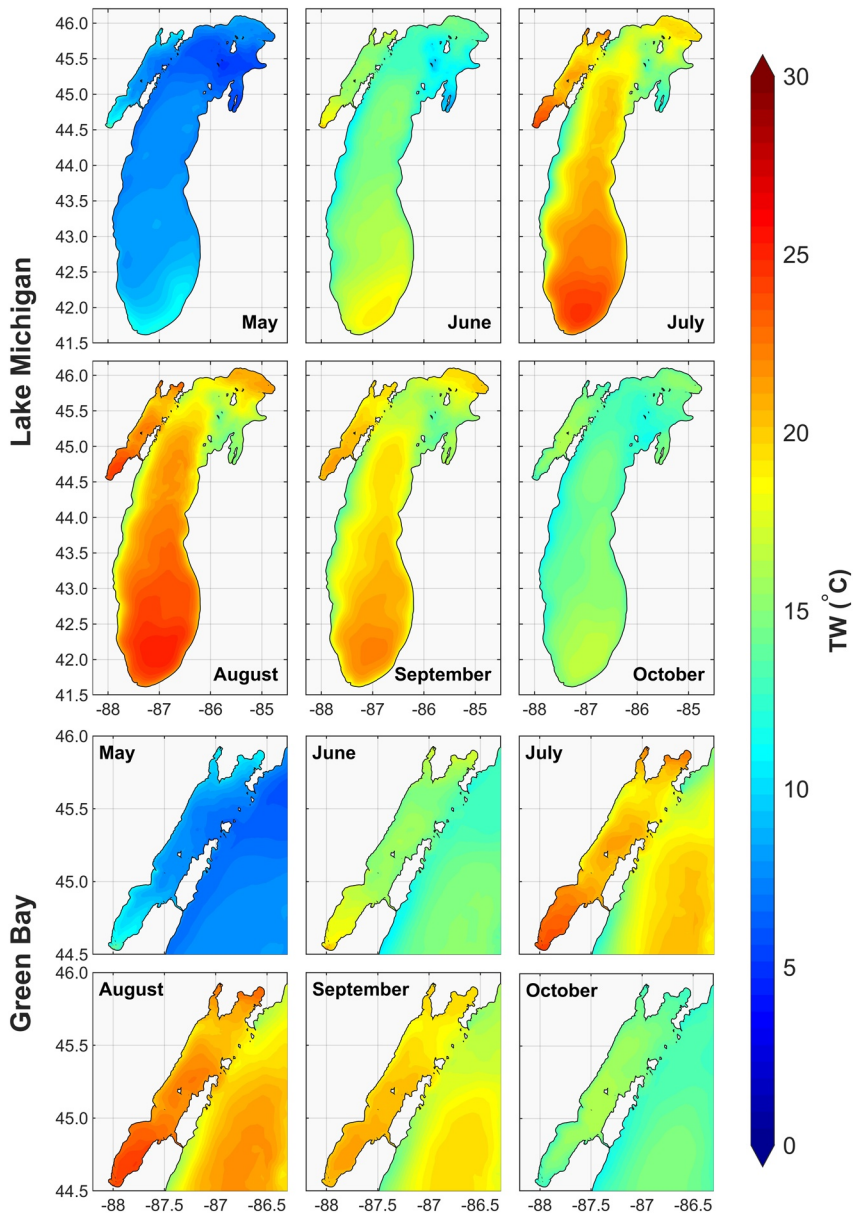

Figure 10. Monthly averaged surface temperature fields (TW) in Lake Michigan and Green Bay during the period of 2016–2019 years.

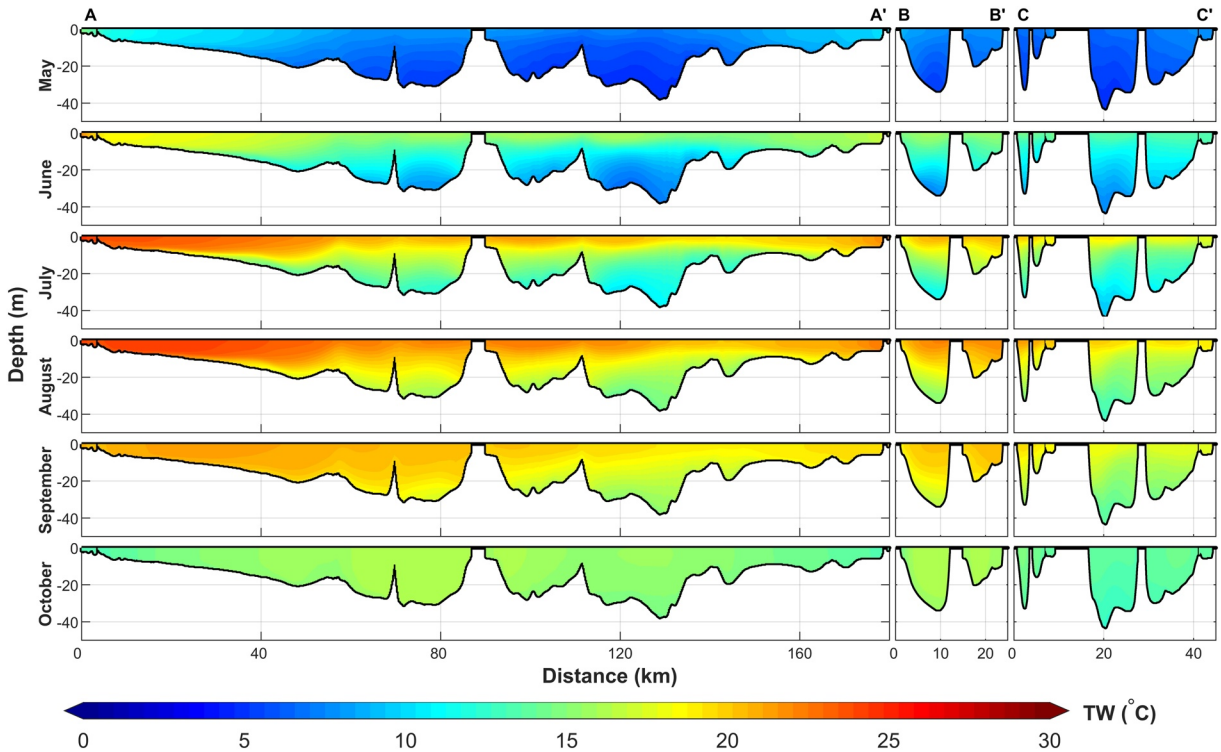

Figure 11. Monthly averaged water temperature (TW) profiles along the A-A' (Green Bay longitudinal axis), B-B' (Chambers Island), and C-C' (connecting straits) cross-sections (as shown in Figure 1) during the period of 2016–2019 years. The vertical axis is exaggerated ~700 times.

lake. Driven by dominant wind direction and coastal upwellings, western nearshore areas of the lake are often slightly colder than the open lake and eastern coastlines. These patterns were also observed by POM-based simulations of thermal structure in Lake Michigan during May–October of 1982–1983 and 1994–1995 (Beletsky & Schwab, 2001). The thermal regime in Green Bay is significantly different than that of Lake Michigan. Warmer temperatures in the bay can be explained by weaker mixing and shallower morphology. July–September are the months with more spatial variability, with higher temperatures in the southern and northern shallow areas, and colder waters near the exchange zone with Lake Michigan, predominantly due to cold water intrusions from the lake.

Stratification is an important aspect of the thermal regime and circulation, and consequently of the ecological functioning of the bay. Figure 11 shows monthly average temperature profiles, based on 2016–2019 simulations, along the three cross-sections shown in Figure 1. The results of this study are consistent with the findings by Hamidi et al. (2015, 2013) and Bravo et al. (2015), showing that stratification in Green Bay starts in June, peaks in July and August, and starts to fade in September, resulting in a duration of about three months. Cross-section A-A' shows that vertical mixing of temperature occurs at faster rates in shallower areas, as expected. The Fox River has a significant influence on the thermal distribution of the southern Green Bay as shown in the first 50 km of the cross-section A-A' temperature profiles, closer to the mouth of the Fox River. Cross-section B-B' shows that the temperature gradient is stronger in the western side channel of Chambers Island section compared to the well-mixed, shallower eastern channel. Stratification patterns are preserved at cross-section C-C', where Green Bay meets Lake Michigan, but with a weaker gradient.

One advantage of FVCOM is its ability to capture upwelling events in coastal areas of Lake Michigan. A comparison of simultaneous wind fields, surface currents, and surface temperature fields indicates that northerly and southerly winds promote upwellings on the western and eastern coastal areas, respectively (Figure S12). This is an important quality when physical models are used to study biogeochemical processes in lake systems.

5.4. Sediment Transport

Figure 12 shows May–October monthly and depth-averaged simulated TSS concentration in Lake Michigan, with higher resolution in Green Bay, based on 2016–2019 simulations. Consistent with shear stress patterns shown in Figure 9, TSS concentration patterns are relatively uniform June through September, with higher concentrations in May and October in the southernmost and northernmost Lake Michigan nearshore areas, as well as southern Green Bay. Periods of resuspension in southwestern Lake Michigan during May are related to wind-driven strong bottom shear stress and the availability of fine-grained sediments in those areas. In almost every month southern Green Bay and southern Lake Michigan experience higher TSS concentrations than the rest of the lake. These patterns are similar to those presented by Lee et al. (2007) for March 1998 episodic events, based on physical simulations of sediment transport and satellite imagery-based maps

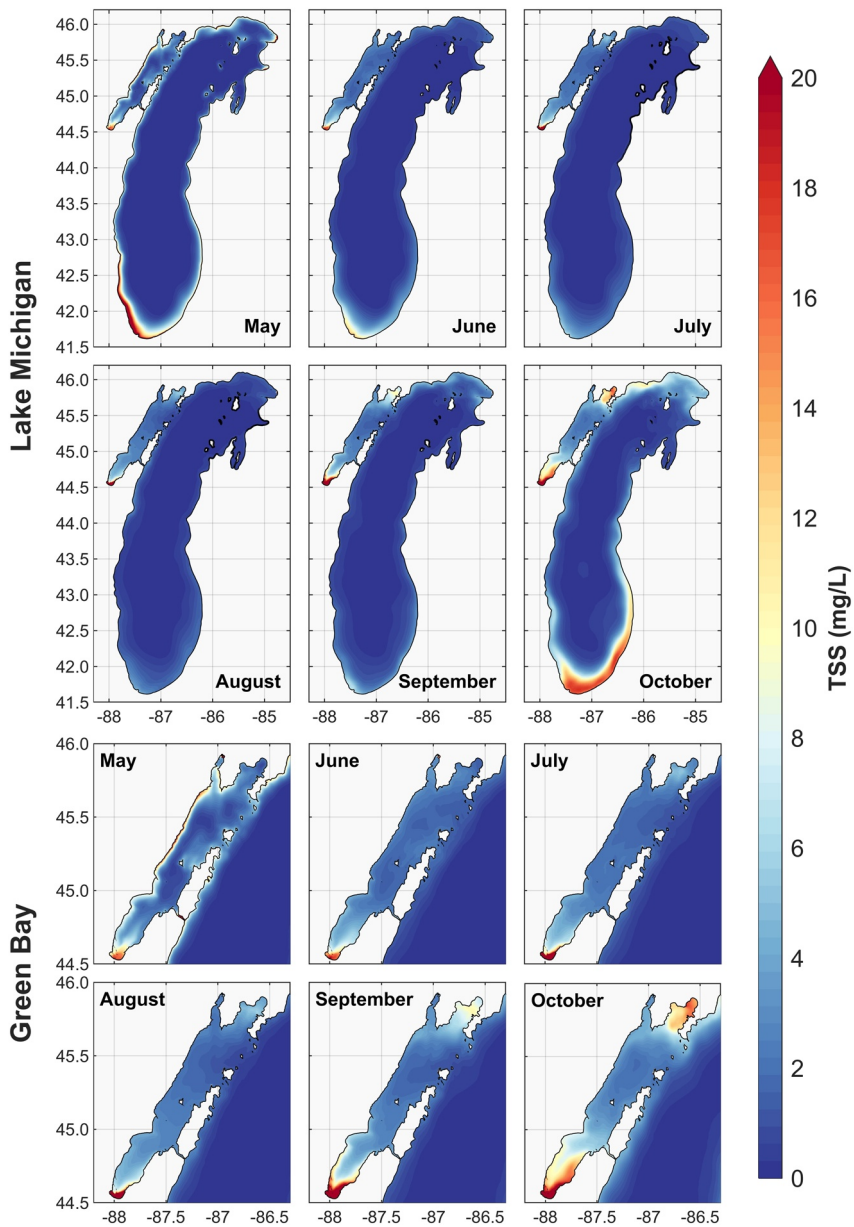

Figure 12. Monthly and depth-averaged total suspended solids (TSS) in Lake Michigan and Green Bay during the period of 2016–2019 years.

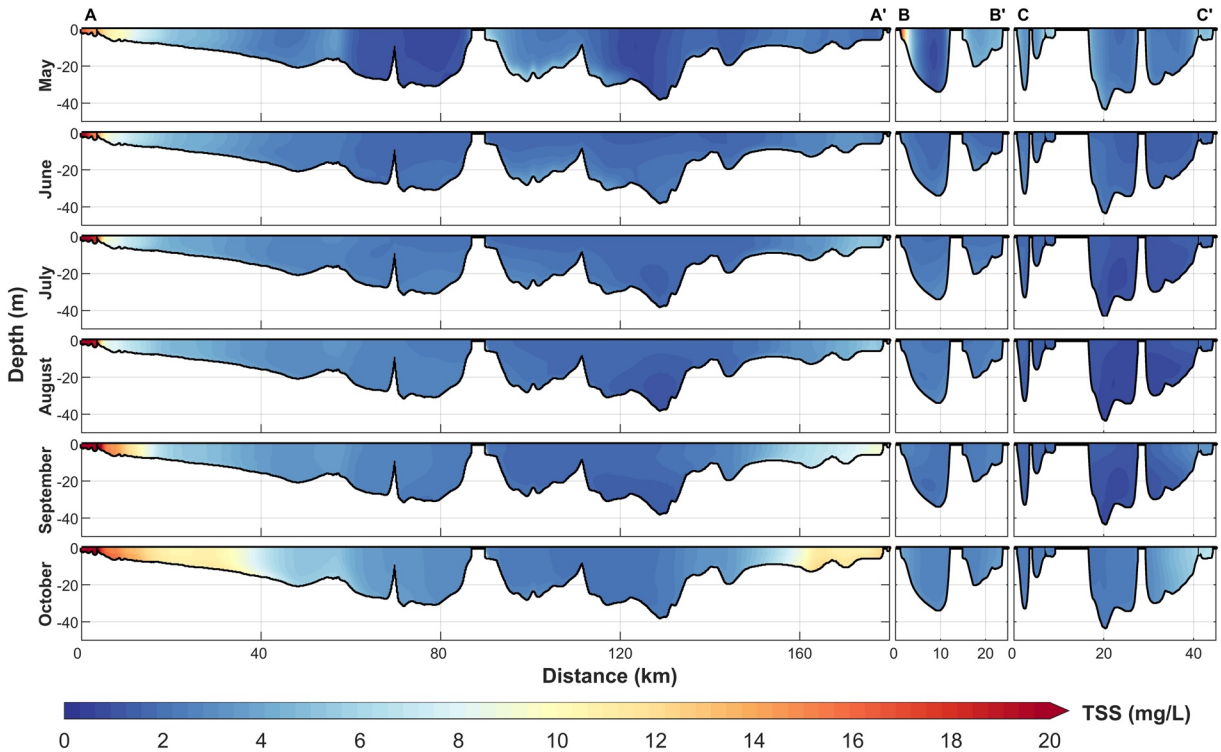

Figure 13. Monthly averaged total suspended solids (TSS) profiles along the A-A' (Green Bay longitudinal axis), B-B' (Chambers Island), and C-C' (connecting straits) cross-sections (as shown in Figure 1) during the period of 2016–2019 years. The vertical axis is exaggerated ~700 times.

of sediment concentration (Figures 8 and 9 in that article). Also, those patterns qualitatively resemble the predicted TSS concentration in southern Lake Michigan during the 1994–1995 period (Lou et al., 2000).

Sediment transport in Green Bay shows significant differences with the transport patterns in Lake Michigan. The Fox River acts as a point source of TSS, and the southern bay shows high TSS concentrations every month, while the northern bay is more influenced by the Lake Michigan patterns of transport. In Upper Green Bay the sediment transport is consistent with shear stress patterns and mostly influenced by circulation and waves. The TSS spatial distribution in the southern bay seems to be governed by the Fox River persistent and significant TSS loading, and by the abundance of fine-grained sediments.

An interesting observation in the patterns of sediment circulation in Green Bay is that TSS concentration is frequently higher in eastern nearshore areas of lower Green Bay, despite higher current-wave driven shear stresses in the western shorelines. One possible explanation is that the river plume tends to flow along the eastern shore because of the frequent counterclockwise circulation in the southern bay driven by wind direction and the Coriolis effect. In addition, several islands in western Green Bay (shown in Figure S2) cause less and/or weaker resuspensions in that area, therefore, the eastern shore contains more sediments, produced mainly by resuspension, than waters near the western shore. That model result is consistent with Klump et al.'s (1997) finding that currents carrying the plume of turbid Fox River water north along the eastern shore of the bay turn westward off Sturgeon Bay in a counterclockwise gyre that leaves behind a blanket of fine slit accumulating at rates of up to ~1 cm/year (160 mg/cm^2/year), 20 times faster than the average for the southern bay as a whole.

The TSS concentration profiles along the A-A' longitudinal cross-section of Green Bay, shown in Figure 13, show more sediment dynamics near the mouth of Fox River (point A) and higher TSS concentrations in the shallow southern and northern ends of the bay at points A and A'. The model results show less variability in TSS concentration at the Chambers Island (B-B') and connecting straits (C-C') cross-sections. Higher sediment concentration west of Chambers Island cross-section (point B) is probably due to stronger currents

near the western shoreline. Results also showed higher sediment transport through channels on the north side of the connecting straits (near point C'), probably due to higher shear stresses in that area.

As we discussed in Section 5.4, combined current-wave actions drive stronger shear stresses at the water-sediment interface, implying more intense resuspension and transport near the bottom. Our analysis showed that on average during the May–October period of 2016–2019 years, considering current-wave combined effects results in 43%, 39%, and 32% higher depth-averaged TSS concentration, respectively, in Lake Michigan, Green Bay, and lower Green Bay in comparison with the case when currents are the sole driver of physical forcing in the lake. TSS patterns in Lake Michigan and Green Bay are illustrated with more details in Figure S11 and Table S2.

5.5. Climatological Summer Circulation and Sediment Transport Patterns in Lake Michigan

This section aims to provide maps of summer transport of heat and sediment in Lake Michigan, based on simulations and using the 2016–2019 meteorological forcing. Figure 14 shows that in general, the prevailing wind direction is southwesterly, and winds are stronger in northern Lake Michigan. The spatial distribution of bottom shear stress shows consistency from year to year, with stronger stresses occurring in southwestern Lake Michigan, Green Bay, and nearshore areas. The maps of surface temperature show a negative, gradual gradient from south to north and a small decline in surface temperature in the southern basin of the lake from 2016 to 2019. The climatological summer surface water temperature in Green Bay was fairly uniform during the simulation period, except that it was somewhat colder near the exchange zone with Lake Michigan.

The map of TSS concentration was fairly steady during the simulation period, but there was a small decrease in TSS concentration in southwestern Lake Michigan from 2016 to 2019. That temporal pattern was consistent with decreasing winds over the southern lake surface during that period. Northern Lake Michigan showed neither temporal variability in TSS patterns nor dependency on wind fields. Those results imply that sediment dynamics in the southern basin is more sensitive to wind and meteorological variability. That is an important pattern to be considered in coastal conservation and shoreline protection.

The maps of TSS concentration showed a different temporal trend in lower Green Bay compared to the whole lake. While TSS concentration showed a decreasing temporal trend in southern Lake Michigan, sediment concentration increased in lower Green Bay between 2016 and 2019. The increase is probably due to increased loading rates into the bay and confirms the importance of including the tributary loads, especially from the Fox River in modeling sediment transport and biogeochemical interactions in Green Bay.

The findings of this research confirm the results of previous studies by showing the importance of wind forcing in the circulation and transport in Lake Michigan. Wind forcing is a primary driver of circulation in Lake Michigan and Green Bay and can influence biogeochemical processes by governing the thermal structure of the lake and the fate and transport of sediments. Wind patterns should be given particular attention in restoration studies for Green Bay.

5.6. Context and Scope of This Research

The 2017 "Summit on the Ecological and Socio-Economic Tradeoffs of Restoration in the Green Bay, Lake Michigan Ecosystem" (Klump et al., 2018) looked at the state of knowledge, gaps, and monitoring needs in the key areas of watershed modeling, biogeochemistry and hydrodynamics, ecosystem modeling and trophic dynamics, habitat and diversity, and socioeconomic and management issues. The introduction of this article summarized the gaps identified in biogeochemistry and hydrodynamics and the intended contribution of this research. This section summarizes previous studies on lake sediment dynamics, resuspension events, biogeochemical interactions, high-turbidity events (due to organic materials, including HABs), and the role of mussels, and considers the potential expansion of this model to study those processes.

Lou et al. (2000) developed a quasi-three-dimensional suspended sediment transport model in Lake Michigan and generalized it to include combined wave-current effects to study bottom sediment resuspension and transport in southern Lake Michigan. In their preliminary application of the model to Lake Michigan, they used only a single grain size to characterize the sedimentary material, and the bottom of the lake is

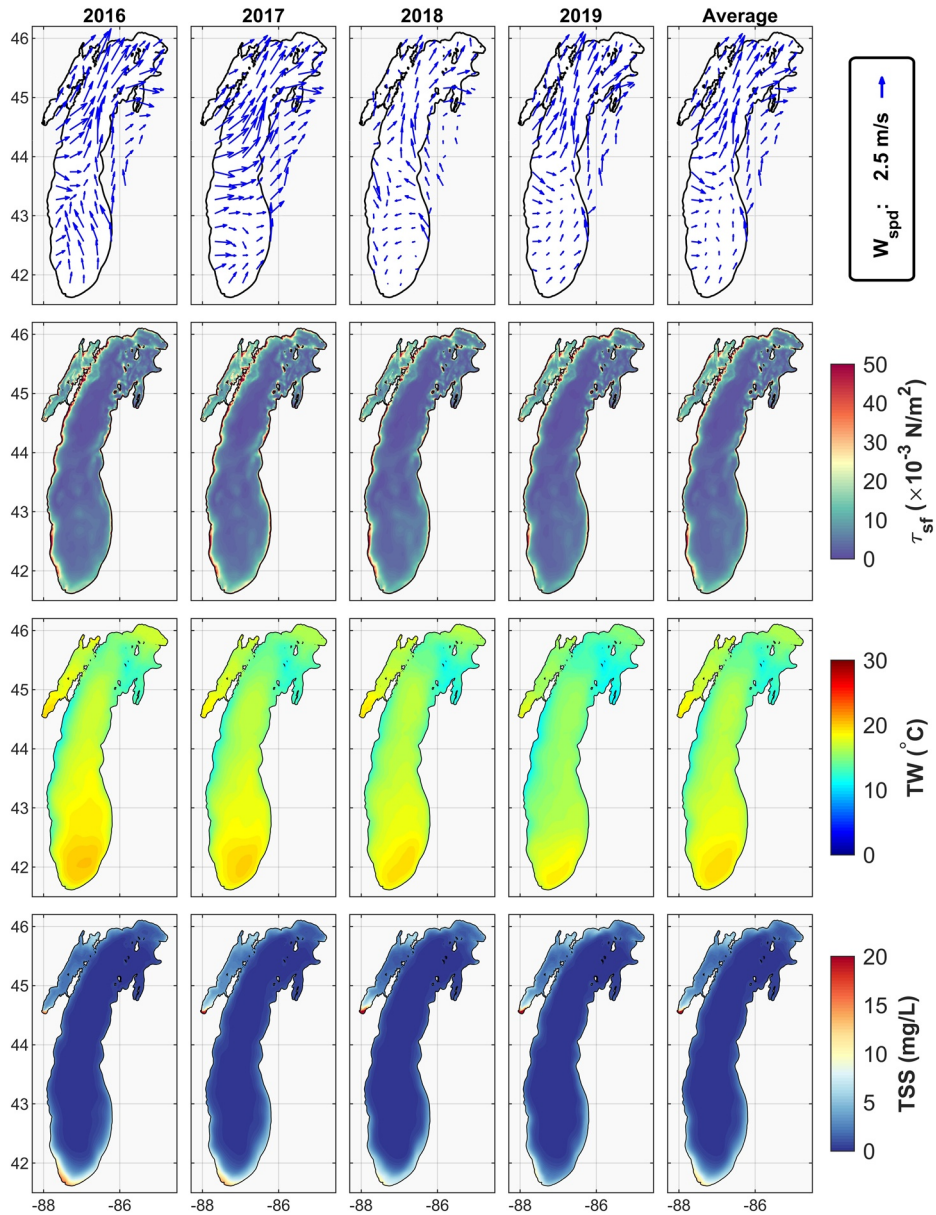

Figure 14. Average annual wind fields (W_{spd}), current-wave driven bottom shear stress (τ_{sf}), surface temperature fields (TW), and depth-averaged total suspended solids (TSS) in Lake Michigan during the May-October period of 2016–2019 years. The last column shows the average for four simulated years.

treated as an unlimited sediment source. They concluded that to improve the model, sediment classifications, spatial bottom sediment distribution, sediment source function, and tributary sediment discharge should be considered. In contrast to Lou et al.'s (2000) model, the present model is fully three-dimensional, accounts for both suspended load and bedload, includes six sediment class sizes ranging from clay to gravel, sediment transport is limited to the mass available in the active layer in each time step, uses a spatial bottom sediment distribution, and includes sediment discharge from the main tributaries to Green Bay, that is, the Fox and Menominee Rivers.

Hawley and Eadie (2007) observed sediment transport in Lake Erie by collecting and analyzing time series measurements of current velocity, wave action, and water transparency at two shallow and deeper sites during the fall and winter of 2004–2005. Their observations at the shallow site showed that bottom resuspension occurred several times during the deployment. Local resuspension did not occur at the deeper

station, yet several advection episodes were observed (advection episodes were not actually measured, but could be simulated by computer models). The organic carbon content at the shallow site was only about 3%, so most of the material collected (probably over 90%) was inorganic. The organic carbon content was even lower at the deeper site (about 0.5%), indicating that even less of the trap material was biogenic in origin. Since no local resuspension was observed at the deeper station, they reasoned that most of the trap material was either bottom sediment resuspended at shallower depths, or material eroded from the bluffs along the northern shoreline.

Valipour et al. (2017) analyzed high-resolution field data, collected in central Lake Erie during April to October of 2008–2009, to investigate the quantitative contribution of sediment resuspension to high-turbidity events. Resuspension events were distinguished within high-turbidity events according to turbidity, fluorescence, and acoustic backscatter time series, as well as satellite images. They observed 16 high-turbidity events, causing a total duration of ~20 days (out of 344 days) with elevated nearbed turbidity (>10 NTU). Of these events, 64% were correlated with algal biomass, with the remaining 18%, 5%, and 4% being attributed to sediment resuspension by surface waves, storm-generated currents, and enhanced nearbed turbulence induced by high frequency internal waves, respectively. The sediment transport model developed in this study was validated using existing measurements of turbidity, acoustic backscatter time series, and satellite images.

Bartlett et al.'s (2018) is the first study of its kind to assess the spatial diversity of cyanotoxins in Green Bay, Lake Michigan. They characterized the diversity and spatial distribution of toxic or otherwise bioactive cyanobacterial peptides (TBPs) in Green Bay. They collected samples during three cruises in August 2014, and July and August 2015 at sites spanning the mouth of the Fox River north to Chambers Island. They found that microcystins (MCs) were positively correlated with Chlorophyll and negatively correlated with distance to the Fox River in all cruises along a well-established south-to-north trophic gradient in Green Bay. The influx of nutrients combined with shallow waters in the lower bay creates an ideal environment for the proliferation of cyanobacteria and the formation of Cyanobacterial harmful algal blooms (cyanoHABs).

Luo et al. (2012) simulated a 1998 spring phytoplankton bloom in Lake Michigan using a coupled physical-biological model. Their biological model was a nutrient-phytoplankton-zooplankton-detritus (NPZD) model, that included phosphorus as the nutrient, phytoplankton, zooplankton, and detritus. The biological model was coupled with the FVCOM physical model and included a wind-wave mixing parametrization but no sediment transport. They searched for the main physical and ecological mechanisms of this spring bloom formation and decay over a long-time scale during March to May, differing from the previous studies of the short-term (5–7 days in March) bloom processes. They confirmed that the phytoplankton bloom was forced by rapidly increasing temperature and light intensity in spring. The thermal front that developed in spring inhibited the transport of nutrients and phytoplankton from the nearshore to the deeper water. The wind-driven gyre circulation in southern Lake Michigan induced significant offshore transport, which contributed to the establishment of the circular bloom. To test the importance of general circulation and interior source of ecological factors in the lake for sustaining the donut-like spring bloom, the phosphorus released from suspended sediments and rivers were excluded from their study.

Nakano and Strayer (2014) summarized the role of biofouling animals, including mussels, in freshwater. The description included the effect of heavy overgrowth and patchy coverage of biofoulers on substrates, how biofoulers can increase turbulence in the water column, increased water clarity, and concentrations of soluble nitrogen and phosphorus. Shen (2016) applied a 1D biophysical model and FVCOM to investigate the ecosystem of Lake Michigan, specifically to explore how invasive mussels affect the nutrient dynamics and distribution of phytoplankton. Wave effects were considered in the 1D biophysical model, but not in the 3D FVCOM simulations. Rowe et al. (2017) used a biophysical model to study the influence of invasive quagga mussels, phosphorus loads, and climate on spatial and temporal patterns of productivity in Lake Michigan. They applied the FVCOM hydrodynamic model, and the FVCOM general ecosystem module (GEM) to implement the NPZD model with the addition of a fifth compartment to represent benthic filter feeder (dreissenid mussel) biomass. They found that although *Chl-a* and primary production declined over the quagga mussel invasion, their results suggested that increased nutrient loads would increase lake-wide productivity even in the presence of mussels; however, altered spatial and temporal patterns of productivity

caused by mussel filter feeding would likely persist. Rowe et al.'s (2017) model included neither a wave model nor a sediment transport model.

Lin et al. (2021) modeled sediment resuspension in Lake Erie by combining the hydrodynamic ELCOM and water quality CAEDYM models. They modeled inorganic particles (e.g., TSS) with the CAEDYM module, by accounting for settling and resuspension, with a three-stage numerical algorithm in ELCOM for scalar transport: (a) vertical mixing by the vertical mixed layer model (Reynolds stress term); (b) advection of the scalar field by the resolved flow field; and (c) horizontal diffusion by turbulent motions. They validated their TSS model qualitatively against turbidity and ADV-amp data at the Central basin in 2009 and at the Central and Eastern basins in 2008 and 2013. In 2008, the model reproduced four high-turbidity events in the Central basin station, but the observed turbidity was continuously high, for more than 10 days, after the fourth event, which was not simulated by the model. Lin et al. (2021) reasoned that settling of phytoplankton during summer in 2008 and 2009 could be the source of sustained high-turbidity. That argument was supported by a spike in *Chl-a* concentration, with a corresponding increase in turbidity. Lin et al.'s (2021) use of the CAEDYM water quality module, which did not simulate the continuously high observed turbidity in the Central basin after the fourth 2008 event, is similar to the sediment transport module FVCOM-SED used in this study.

Lin et al. (2021) described Lake Erie as comprised of western, central, and eastern basins, with maximum depths of 16, 25, and 64 m, respectively. The shallowness of the western and central basins makes them susceptible to resuspension of sediments by wind-induced surface waves. Lake Michigan, Green Bay, and lower Green Bay have maximum depths of 282, 53, and 30 m, respectively. While Western Lake Michigan is river dominated (tributary rivers discharge 5,246 m^3/s), Green Bay is subject to extensive water mass exchange with Lake Michigan at its northern end, and lower Green Bay receives tributaries discharges of 329 m^3/s.

Niu et al. (2018) investigated the contributions of river-loaded versus resuspended sediments to high-turbidity events in Western Lake Erie during ice-free cycles, using FVCOM, FVCOM-SWAVE, and FVCOM-SED. The relative contributions of sediment actions to high-turbidity events in Green Bay are different from those in Western Lake Erie because of contrasts in the geophysical characteristics (e.g., depths), wind forcing, extensive water exchange with Lake Michigan and typical two-layer flows, and thermal regime. Niu et al. (2018) found distinctive seasonal variations in wind forcing and sediment dynamics in Western Lake Erie between spring (April–May), summer (June–August), and fall (October–November). Monthly averaged wind over Green Bay rotates in June from the northeast to the southwest and maintains the same general direction for the rest of the summer, driving typical two-layer flows with cold water intrusions from Lake Michigan (Hamidi et al., 2015). Those contrasts differentiate the present application of FVCOM-SWAN-SED from Niu et al.'s (2018) application. Regarding the detailed implementation of the FVCOM-SWAN-SED model, there are significant differences between Niu et al.'s (2018) and the present implementation. While Niu et al. (2018) sediment model used a uniform distribution of cohesive bed sediments, the current study improved the physical description of the system by implementing a non-uniform distribution of mixed bed materials (cohesive and non-cohesive) in the description of bottom sediments. Whereas Niu et al. (2018) used the Coupled Ocean Atmosphere Response Experiment (COARE) flux algorithm in their Lake Erie model, in this study heat flux is calculated using the FVCOM SOLAR approach developed by NOAA/GLERL for application in the GLCFS models (NOAA, 2021b).

Valipour et al. (2016) developed a high-resolution three-dimensional water quality model for Lake Erie capable of resolving predominant physical processes to study nutrient dynamics, with a particular emphasis on the northern nearshore region of Lake Erie's eastern basin. The lake model output in conjunction with the *Cladophora* growth model (CGM) was used to predict *Cladophora* growth. The models were validated using extensive nearshore water quality, *Cladophora* biomass, and tissue phosphorus measurements collected during April–September of 2013. Together, the models were used to evaluate the response of nearshore phosphorus concentrations and *Cladophora* growth due to changes in external phosphorus loading.

Bravo et al. (2020) linked a previously built hydrodynamic model and a water quality model developed by Fillingham (2015), extended to three dimensions to simulate the transport and fate of phosphorus in the nearshore area of Lake Michigan. Their model accounted for the interactions between phosphorus, *Cladophora*, mussels, and lake sediments in the nearshore zone. They quantified the lake assimilative capacity

by applying their model to estimate the area required for mixing and diluting wastewater treatment plant outfall total phosphorus loadings to the level of the lake target concentration during the *Cladophora* growing season. Their model results compared well with empirical measurements of particulate and dissolved phosphorus as well as *Cladophora* biomass and phosphorus content. The model was applied to test scenarios of wastewater treatment plant phosphorus loading in two different years, in order to help establish phosphorus discharge limits for the plant.

The stage is set to apply the approach developed in this study, which includes wave and sediment transport simulation, as follows: (a) to investigate high-turbidity events (due to organic materials including HABs); (b) to study algal blooms in lakes following Luo et al.'s (2012) coupled physical-biological modeling approach; (c) to improve the study of the influence of invasive dreissenid mussels on lakes ecosystems pursuing Rowe et al.'s (2017) modeling methods; and (d) to study the interactions between phosphorus, *Cladophora*, mussels, and lake sediments by using the biophysical concepts developed by Bravo et al. (2019).

Ongoing research will apply the model to: (a) to evaluate sediment dynamics in the bay under different climate conditions and loading scenarios in river/watershed management; (b) predicting the short- and long-term effects of the Cat Island Chain restoration in altering flow, transport, deposition, and benthic habitat in the area of concern (AOC); and (c) to establish a sediment budget for lower- and entire Green Bay. One of the principal goals of the Cat Island Chain restoration project was to reestablish a barrier island complex and reduce wave energy in the inner bay as a means of reducing resuspension and increasing water clarity.

6. Conclusions

The hydrodynamic, wind-wave, and sediment transport model developed in this study includes in a single platform of all the relevant geophysical drivers, namely the momentum flux generated by wind, the heat flux across the water surface, the Earth's rotation, thermal stratification, and topography. The single model of Lake Michigan and its Green Bay estuary has high resolution in the bay and in the exchange zone between the open lake and the bay. The single-model approach provides the desired resolution in the bay estuary and represents the combined effects of tributary flows and lake intrusions. The model overcomes limitations of previous nested models of the estuary that used potentially problematic open boundary conditions to represent the exchange of mass, energy, and momentum with Lake Michigan, and of previous whole-lake models that lacked the desired high resolution in the bay or did not include physically based wind-wave and sediment transport modules. The model confirms the findings of previous studies on Lake Michigan and demonstrates how the circulation, thermal regime, wind action, and sediment transport in the Green Bay estuary depend on meteorological forcing, tributary flows, and lake water intrusions.

Winds are a primary driver of circulation and wave action in Lake Michigan. Eastern winds dominate in May-June, and the wind fields shift to southwesterly and southerly directions in July until October, when winds are the strongest. Cyclonic (counterclockwise) circulation dominates Lake Michigan, and the formation of gyres is more common in the southern basin. In consistency with wind patterns, circulation is weaker in May and currents accelerate starting in June. Wave action in Lake Michigan is limited in May–August, gradually increases in September, and escalates in October. The northern basin of Lake Michigan experiences stronger waves due to dominant southern winds. Winds drive the fluxes of water, heat, and sediment between the lake and the estuary. In Green Bay, the currents show more spatial variability than the wind fields, with widespread formation of gyres. Surface currents in Green Bay flow predominantly north (especially near the shorelines) and bottom currents flow predominantly toward the south, providing evidence that the interaction of tributary flows and lake currents force summertime stratified flow conditions in the bay. In concert with Lake Michigan, waves in the bay are stronger in September and October. Upper Green Bay and the exchange zone experience stronger waves due to rapid change in the bottom elevation in that area.

The southern basin of Lake Michigan is generally warmer than the rest of the lake. Driven by dominant wind direction and coastal upwellings, western nearshore areas of the lake are often slightly colder than the open lake and eastern coastlines. Analysis of simultaneous wind fields, surface currents, and surface temperature fields indicates that northerly and southerly winds promote upwellings on the western and eastern coastal areas, respectively. The model's ability to capture upwelling events is an important quality in the

study of biogeochemical processes in lake systems. Warmer temperatures in the bay are explained by weaker mixing and shallower morphology. Stratification in Green Bay starts in June, peaks in July and August, and starts to fade in September, resulting in a duration of about three months. Field data and model results showed that the Fox River has a significant influence on the thermal distribution of southern Green Bay.

Total suspended sediment (TSS) concentration fields in Lake Michigan are relatively uniform June through September, concentrations are higher in May and October in the southernmost and northernmost Lake Michigan nearshore areas, and in southern Green Bay. Sediment transport in the estuary is clearly shaped by both tributary loads and exchanges with Lake Michigan. The southern bay shows high TSS concentrations because the Fox River acts as a main point source of sediments. The Fox River plume tends to flow along the eastern shore because of counterclockwise circulation in the southern bay driven by wind direction and the Coriolis effect, and consequently, TSS concentration is normally higher in the eastern nearshore areas of lower Green Bay. Upper Green Bay is more influenced by current and wave exchanges with Lake Michigan. Sediment transport is higher through the channels on the north side of the connecting straits, because of higher shear stresses in that area.

Data Availability Statement

Lake Michigan bathymetry and shoreline data are obtained from NOAA National Geophysical Data Center (http://maps.ngdc.noaa.gov/viewers/bathymetry/). Input meteorological forcing data are based on NOAA National Centers for Environmental Information (https://www.ncei.noaa.gov/). Buoy observations were also downloaded from NOAA National Data Buoy Center (https://www.ndbc.noaa.gov/), Great Lakes Observing System (https://uwm.edu/glos/), *lakestat* monitoring program (http://www.lakestat.com/), and USGS National Water Information System (NWIS) database (https://waterdata.usgs.gov/nwis). River inputs are also based on the USGS NWIS database. Lake Michigan water level data is downloaded from NOAA Tides and Currents data set (https://tidesandcurrents.noaa.gov/stations.html?type=Water+Levels). Turbidity and TSS in situ observations at the mouth of Fox River are provided based on personal communications with Dr. Sarah Bartlett at the NEW Water (http://newwater.us/programs-initiatives/aquatic-monitoring-program/). MODIS imagery products are obtained from the NASA EARTHDATA platform (https://earthdata.nasa.gov/).

Acknowledgments
This project was funded partially by the University of Wisconsin Sea Grant Omnibus Program Grant 144-AAG3496-UWMKE19A. We appreciate Jeff Houghton for assistance in the fieldwork, Jim Wagner and Jason Bacon for IT support, and Jessie Grow, Dr. Sarah Bartlett, and Dr. Todd Miller for providing field data in Green Bay and Lake Michigan. This is GLERL contribution 1991.

References

Anderson, E. J., & Phanikumar, M. S. (2011). Surface storage dynamics in large rivers: Comparing three-dimensional particle transport, one-dimensional fractional derivative, and multirate transient storage models. *Water Resources Research*, *47*(9). https://doi.org/10.1029/2010WR010228

Anderson, E. J., & Schwab, D. J. (2011). Relationships between wind-driven and hydraulic flow in Lake St. Clair and the St. Clair River Delta. *Journal of Great Lakes Research*, *37*(1), 147–158. https://doi.org/10.1016/J.JGLR.2010.11.007

Anderson, E. J., & Schwab, D. J. (2013). Predicting the oscillating bi-directional exchange flow in the Straits of Mackinac. *Journal of Great Lakes Research*, *39*(4), 663–671. https://doi.org/10.1016/j.jglr.2013.09.001

Anderson, E. J., Schwab, D. J., & Lang, G. A. (2010). Real-Time Hydraulic and Hydrodynamic Model of the St. Clair River, Lake St. Clair, Detroit River System. *Journal of Hydraulic Engineering*, *136*(8), 507–518. https://doi.org/10.1061/(ASCE)HY.1943-7900.0000203

Anderson, E. J., Stow, C. A., Gronewold, A. D., Mason, L. A., McCormick, M. J., Qian, S. S., et al. (2021). Seasonal overturn and stratification changes drive deep-water warming in one of Earth's largest lakes. *Nature Communications*, *12*(1), 1688. https://doi.org/10.1038/s41467-021-21971-1

Ariathurai, R., & Arulanandan, K. (1978). Erosion rates of cohesive soils. *Journal of the Hydraulics Division*, *101*(5), 635–639. https://doi.org/10.1061/jyceaj.0004937

Bai, X., Wang, J., Schwab, D. J., Yang, Y., Luo, L., Leshkevich, G. A., & Liu, S. (2013). Modeling 1993–2008 climatology of seasonal general circulation and thermal structure in the Great Lakes using FVCOM. *Ocean Modelling*, *65*, 40–63. https://doi.org/10.1016/J.OCEMOD.2013.02.003

Bartlett, S. L., Brunner, S. L., Klump, J. V., Houghton, E. M., & Miller, T. R. (2018). Spatial analysis of toxic or otherwise bioactive cyanobacterial peptides in Green Bay, Lake Michigan. *Journal of Great Lakes Research*, *44*(5), 924–933. https://doi.org/10.1016/j.jglr.2018.08.016

Battjes, J. A., & Janssen, J. P. F. M. (1978). Energy loss and set-up due to breaking of random waves. In *Coastal engineering 1978* (pp. 569–587). American Society of Civil Engineers. https://doi.org/10.1061/9780872621909.034

Beletsky, D., O'Connor, W. P., Schwab, D. J., Dietrich, D. E. (1997). Numerical Simulation of Internal Kelvin Waves and Coastal Upwelling Fronts*. *Journal of Physical Oceanography*, *27*, (7), 1197–1215. http://doi.org/10.1175/1520-0485(1997)027<1197:nsoikw>2.0.co;2

Beletsky, D., Schwab, D., & McCormick, M. (2006). Modeling the 1998-2003 summer circulation and thermal structure in Lake Michigan. *Journal of Geophysical Research*, *111*(10), 1–18. https://doi.org/10.1029/2005JC003222

Beletsky, D., & Schwab, D. J. (2001). Modeling circulation and thermal structure in Lake Michigan: Annual cycle and interannual variability. *Journal of Geophysical Research: Oceans*, *106*(C9), 19745–19771. https://doi.org/10.1029/2000JC000691

Beletsky, D., Schwab, D. J., Roebber, P. J., McCormick, M. J., Miller, G. S., & Saylor, J. H. (2003). Modeling wind-driven circulation during the March 1998 sediment resuspension event in Lake Michigan. *Journal of Geophysical Research*, *108*(C2). https://doi.org/10.1029/2001jc001159

Booij, N., Haagsma, I. J. G., Holthuijsen, L. H., Kieftenburg, A. T. M. M., Ris, R. C., van der Westhuysen, A. J., & Zijlema, M. (2004). *SWAN Cycle III version 40.51 Technical documentation*.

Booij, N., Ris, R. C., & Holthuijsen, L. H. (1999). A third-generation wave model for coastal regions: 1. Model description and validation. *Journal of Geophysical Research*, *104*(C4), 7649–7666. https://doi.org/10.1029/98JC02622

Bravo, H. R., Bootsma, H., & Khazaei, B. (2019). Fate of phosphorus from a point source in the Lake Michigan nearshore zone. *Journal of Great Lakes Research*, *45*, 1182–1196. https://doi.org/10.1016/j.jglr.2019.09.007

Bravo, H. R., Hamidi, S. A., Anderson, E. J., Klump, J. V., & Khazaei, B. (2020). Timescales of transport through lower Green Bay. *Journal of Great Lakes Research*. https://doi.org/10.1016/j.jglr.2020.06.010

Bravo, H. R., Hamidi, S. A., Klump, J. V., & Waples, J. T. (2015). Currents and heat fluxes induce stratification leading to hypoxia in Green Bay, Lake Michigan. In *E-proceedings of the 36th IAHR World Congress, (1985)* (pp. 1–10).

Bravo, H. R., Hamidi, S. A., Klump, J. V., & Waples, J. T. (2017). Physical drivers of the circulation and thermal regime impacting seasonal hypoxia in Green Bay, Lake Michigan. In *Modeling coastal hypoxia* (pp. 23–47). Springer International Publishing. https://doi.org/10.1007/978-3-319-54571-4_2

Chen, C., Beardsley, R. C., Cowles, G., Qi, J., Lai, Z., Gao, G., et al. (2013). *An unstructured grid, finite-volume Community Ocean model FVCOM user manual*. Retrieved from http://fvcom.smast.umassd.edu/

Chen, C., Huang, H., Beardsley, R. C., Liu, H., Xu, Q., & Cowles, G. (2007). A finite volume numerical approach for coastal ocean circulation studies: Comparisons with finite difference models. *Journal of Geophysical Research*, *112*(C3), C03018. https://doi.org/10.1029/2006JC003485

Chen, C., Liu, H., & Beardsley, R. C. (2003). An unstructured grid, finite-volume, three-dimensional, primitive equations ocean model: Application to coastal ocean and estuaries. *Journal of Atmospheric and Oceanic Technology*, *20*(1), 159–186. https://doi.org/10.1175/1520-0426(2003)020<0159:augfvt>2.0.co;2

Chen, C., Wang, L., Ji, R., Budd, J. W., Schwab, D. J., Beletsky, D., et al. (2004). Impacts of suspended sediment on the ecosystem in Lake Michigan: A comparison between the 1998 and 1999 plume events. *Journal of Geophysical Research*, *109*(C10), C10S05. https://doi.org/10.1029/2002JC001687

Chen, T., Zhang, Q., Wu, Y., Ji, C., Yang, J., & Liu, G. (2018). Development of a wave-current model through coupling of FVCOM and SWAN. *Ocean Engineering*, *164*, 443–454. https://doi.org/10.1016/J.OCEANENG.2018.06.062

Cotton, G. F. (1979). ARL models of global solar radiation. In Hourly solar radiation-surface meteorological observations (Final Rep. TD-9724, SOLMET, Vol. 2). Natl. Clim. Data Cent.

Deines, K. L. (1999). Backscatter estimation using broadband acoustic Doppler current profilers. In *Proceedings of the IEEE Working Conference on Current Measurement* (pp. 249–253). https://doi.org/10.1109/ccm.1999.755249

Eadie, B. J., Bell, G. L., & Hawley, N. (1991). *Sediment trap study in the Green Bay mass balance program: Mass and organic carbon fluxes, resuspension, and particle settling velocities* (NOAA Technical Memorandum ERL GLERL-75). Great Lakes Environmental Research Laboratory.

Fillingham, J. (2015). *Modeling Lake Michigan nearshore carbon and phosphorus dynamics theses and dissertations*. University of Wisconsin-Milwaukee. Retrieved from http://dc.uwm.edu/etd/871

García, M. H. (2008). Sediment Transport and Morphodynamics. In M. H. García (Ed.), *Sedimentation engineering: Processes, measurements, modeling, and practice* (pp. 21–163). American Society of Civil Engineers. https://doi.org/10.1061/9780784408148.ch02

Ge, J., Torres, R., Chen, C., Liu, J., Xu, Y., Bellerby, R., et al. (2020). Influence of suspended sediment front on nutrients and phytoplankton dynamics off the Changjiang Estuary: A FVCOM-ERSEM coupled model experiment. *Journal of Marine Systems*, *204*, 103292. https://doi.org/10.1016/j.jmarsys.2019.103292

GLOS. (2021). *Data | Great lakes observing system*. Retrieved from https://uwm.edu/glos/data/

Grunert, B. K., Brunner, S. L., Hamidi, S. A., Bravo, H. R., & Klump, J. V. (2018). Quantifying the influence of cold water intrusions in a shallow, coastal system across contrasting years: Green Bay, Lake Michigan. *Journal of Great Lakes Research*, *44*(5), 851–863. https://doi.org/10.1016/J.JGLR.2018.07.009

Guerra, M., Cienfuegos, R., Thomson, J., & Suarez, L. (2017). Tidal energy resource characterization in Chacao Channel, Chile. *International Journal of Marine Energy*, *20*, 1–16. https://doi.org/10.1016/J.IJOME.2017.11.002

Guttman, N. B., & Matthews, J. D. (1979). Computation of extraterrestrial solar radiation, solar elevation angle, and true solar time of sun- rise and sunset. In *Hourly solar radiation-surface meteorological observations* (Final Rep. TD-9724, SOLMET, Vol. 2). Natl. Clim. Data Cent.

Hamidi, S. A., Bravo, H. R., & Klump, J. V. (2013). Evidence of multiple physical drivers on the circulation and thermal regime in the Green Bay of Lake Michigan. In *World environmental and Water Resources Congress 2013* (pp. 1719–1726). American Society of Civil Engineers. https://doi.org/10.1061/9780784412947.169

Hamidi, S. A., Bravo, H. R., Val Klump, J., & Waples, J. T. (2015). The role of circulation and heat fluxes in the formation of stratification leading to hypoxia in Green Bay, Lake Michigan. *Journal of Great Lakes Research*, *41*(4), 1024–1036. https://doi.org/10.1016/j.jglr.2015.08.007

Hamidi, S. A., Hosseiny, H., Ekhtari, N., & Khazaei, B. (2017). Using MODIS remote sensing data for mapping the spatio-temporal variability of water quality and river turbid plume. *Journal of Coastal Conservation*, *21*(6), 939–950. https://doi.org/10.1007/s11852-017-0564-y

Harris, C. K., & Wiberg, P. L. (2001). A two-dimensional, time-dependent model of suspended sediment transport and bed reworking for continental shelves. *Computers & Geosciences*, *27*(6), 675–690. https://doi.org/10.1016/S0098-3004(00)00122-9

Harris, V. A., & Christie, J. (1987). The lower Green Bay remedial action plan: Nutrient and eutrophication management. In *Technical advisory committee report, publication no. WR-167-87*. Wisconsin Department of Natural Resources.

Hasselmann, K., Barnett, T. P., Bouws, E., Carlson, H. K., Cartwright, D. E., Enke, K., et al. (1973). *Measurements of wind-wave growth and swell decay during the Joint North sea wave project (JONSWAP)*.

Hasselmann, S., Hasselmann, K., Allender, J. H., & Barnett, T. P. (1985). Computations and parameterizations of the nonlinear energy transfer in a gravity-wave spectrum. Part II: Parameterizations of the nonlinear energy transfer for application in wave models. *Journal of Physical Oceanography*, *15*(11), 1378–1391. https://doi.org/10.1175/1520-0485(1985)015<1378:capotn>2.0.co;2

Hawley, N., & Eadie, B. J. (2007). Observations of sediment transport in Lake Erie during the Winter of 2004–2005. *Journal of Great Lakes Research*, *33*(4), 816–827. https://doi.org/10.3394/0380-1330(2007)33[816:oostil]2.0.co;2

Hawley, N., Lesht, B. M., & Schwab, D. J. (2004). A comparison of observed and modeled surface waves in southern Lake Michigan and the implications for models of sediment resuspension. *Journal of Geophysical Research*, *109*(C10), C10S03. https://doi.org/10.1029/2002JC001592

Hawley, N., & Niester, J. (1993). Measurement of horizontal sediment transport in Green Bay, May-October, 1989. *Journal of Great Lakes Research*, *19*(2), 368–378. https://doi.org/10.1016/S0380-1330(93)71225-3

Huang, H., Chen, C., Cowles, G. W., Winant, C. D., Beardsley, R. C., Hedstrom, K. S., & Haidvogel, D. B. (2008). FVCOM validation experiments: Comparisons with ROMS for three idealized barotropic test problems. *Journal of Geophysical Research*, *113*(C7), C07042. https://doi.org/10.1029/2007JC004557

HydroQual Inc. (1999). *Hydrodynamics, sediment transport, and sorbent dynamics in Green Bay*. Report to Wisconsin Department of Natural Resources. https://semspub.epa.gov/work/05/417180.pdf

Ivanoff, A. (1977). Oceanic absorption of solar energy. In E. B. Kraus (Ed.), *Modelling and prediction of the upper layers of the ocean* (pp. 47–72). Pergamon. Retrieved from https://ci.nii.ac.jp/naid/10003519602/

Ji, R., Chen, C., Budd, J. W., Schwab, D. J., Beletsky, D., Fahnenstiel, G. L., et al. (2002). Influences of suspended sediments on the ecosystem in Lake Michigan: A 3-D coupled bio-physical modeling experiment. *Ecological Modelling*, *152*(2–3), 169–190. https://doi.org/10.1016/S0304-3800(02)00027-3

Jones, C. A. (2000). *An accurate model of sediment transport*. University of California.

Kaster, J. L., Groff, C. M., Klump, J. V., Rupp, D. L., Iyer, S., Hansen, A., et al. (2018). Evaluation of lower Green Bay benthic fauna with emphasis on re-ecesis of Hexagenia mayfly nymphs. *Journal of Great Lakes Research*, *44*(5), 895–909. https://doi.org/10.1016/J.JGLR.2018.06.006

Khazaei, B. (2020). *Development of a hydrodynamic and sediment transport model for Green Bay*. University of Wisconsin-Milwaukee. https://dc.uwm.edu/etd/2392/

Khazaei, B., Hamidi, S. A., & Nabizadeh, A. (2018). An empirical approach to estimate total suspended sediment using observational data in Fox River and Southern Green Bay, WI. In *World Environmental and Water Resources Congress*. https://doi.org/10.1061/9780784481424.005

Khazaei, B., & Wu, C. (2018). Estimation of vegetation coverage based on seasonal variabilities in MODIS-based vegetation indices. In *World Environmental and Water Resources Congress 2018* (pp. 11–20). American Society of Civil Engineers. https://doi.org/10.1061/9780784481400.002

Klump, J. V., Brunner, S. L., Grunert, B. K., Kaster, J. L., Weckerly, K., Houghton, E. M., et al. (2018). Evidence of persistent, recurring summertime hypoxia in Green Bay, Lake Michigan. *Journal of Great Lakes Research*, *44*(5), 841–850. https://doi.org/10.1016/J.JGLR.2018.07.012

Klump, J. V., Bratton, J., Fermanich, K., Forsythe, P., Harris, H. J., Howe, R. W., & Kaster, J. L. (2018). Green Bay, Lake Michigan: A proving ground for Great Lakes restoration. *Journal of Great Lakes Research*, *44*(5), 825–828. https://doi.org/10.1016/J.JGLR.2018.08.002

Klump, J. V., Fitzgerald, S. A., & Waplesa, J. T. (2009). Benthic biogeochemical cycling, nutrient stoichiometry, and carbon and nitrogen mass balances in a eutrophic freshwater bay. *Limnology & Oceanography*, *54*(3), 692–712. https://doi.org/10.4319/lo.2009.54.3.0692

Klump, J. V., Edgington, D. N. N., Sager, P. E. E., & Robertson, D. M. M. (1997). Sedimentary phosphorus cycling and a phosphorus mass balance for the Green Bay (Lake Michigan) ecosystem. *Canadian Journal of Fisheries and Aquatic Sciences*, *54*(1), 10–26. https://doi.org/10.1139/f96-247

Komen, G. J., Hasselmann, K., & Hasselmann, K. (1984). On the existence of a fully developed wind-sea spectrum. *Journal of Physical Oceanography*, *14*(8), 1271–1285. https://doi.org/10.1175/1520-0485(1984)014<1271:oteoaf>2.0.co;2

Labuhn, S. L. (2017). *Dissolved oxygen dynamics within Green Bay in an effort to understand hypoxia Table of Contents*. University of Wisconsin-Milwaukee.

Lai, W., Pan, J., & Devlin, A. T. (2018). Impact of tides and winds on estuarine circulation in the Pearl River Estuary. *Continental Shelf Research*, *168*, 68–82. https://doi.org/10.1016/J.CSR.2018.09.004

Le Hir, P., Cayocca, F., & Waeles, B. (2011). Dynamics of sand and mud mixtures: A multiprocess-based modelling strategy. *Continental Shelf Research*, *31*(10 SUPPL), S135–S149. https://doi.org/10.1016/j.csr.2010.12.009

Lee, C., Schwab, D. J., Beletsky, D., Stroud, J., & Lesht, B. (2007). Numerical modeling of mixed sediment resuspension, transport, and deposition during the March 1998 episodic events in southern Lake Michigan. *Journal of Geophysical Research: Oceans*, *112*(2), 1–17. https://doi.org/10.1029/2005JC003419

Lee, C., Schwab, D. J., & Hawley, N. (2005). Sensitivity analysis of sediment resuspension parameters in coastal area of southern Lake Michigan. *Journal of Geophysical Research C: Oceans*, *110*(3), 1–16. https://doi.org/10.1029/2004JC002326

Li, B., Tanaka, K. R., Chen, Y., Brady, D. C., & Thomas, A. C. (2017). Assessing the quality of bottom water temperatures from the Finite-Volume Community Ocean Model (FVCOM) in the Northwest Atlantic Shelf region. *Journal of Marine Systems*, *173*, 21–30. https://doi.org/10.1016/J.JMARSYS.2017.04.001

Li, J., Pan, S., Chen, Y., Fan, Y.-M., & Pan, Y. (2018). Numerical estimation of extreme waves and surges over the northwest Pacific Ocean. *Ocean Engineering*, *153*, 225–241. https://doi.org/10.1016/J.OCEANENG.2018.01.076

Lin, S., Boegman, L., Valipour, R., Bouffard, D., Ackerman, J. D., & Zhao, Y. (2021). Three-dimensional modeling of sediment resuspension in a large shallow lake. *Journal of Great Lakes Research*, *47*(4), 970–984. https://doi.org/10.1016/J.JGLR.2021.04.014

Lou, J., Schwab, D. J., Beletsky, D., & Hawley, N. (2000). A model of sediment resuspension and transport dynamics in southern Lake Michigan. *Journal of Geophysical Research*, *105*(C3), 6591–6610. https://doi.org/10.1029/1999JC900325

Luo, L., Wang, J., Schwab, D. J., Vanderploeg, H., Leshkevich, G., Bai, X., et al. (2012). Simulating the 1998 spring bloom in Lake Michigan using a coupled physical-biological model. *Journal of Geophysical Research*, *117*, 10011. https://doi.org/10.1029/2012JC008216

Manchester-Neesvig, J. B., Andren, A. W., & Edgington, D. N. (1996). Patterns of mass sedimentation and of deposition of sediment contaminated by PCBs in Green Bay. *Journal of Great Lakes Research*, *22*(2), 444–462. https://doi.org/10.1016/S0380-1330(96)70969-3

Mantz, P. A. (1977). Incipient transport of fine grains and flakes by fluids-extended Shields diagram. *Journal of the Hydraulics Division*, *103*(HY6). https://doi.org/10.1061/jyceaj.0004766

Mao, M., van der Westhuysen, A. J., Xia, M., Schwab, D. J., & Chawla, A. (2016). Modeling wind waves from deep to shallow waters in Lake Michigan using unstructured SWAN. *Journal of Geophysical Research: Oceans*, *121*(6), 3836–3865. https://doi.org/10.1002/2015JC011340

Mao, M., & Xia, M. (2017). Dynamics of wave–current–surge interactions in Lake Michigan: A model comparison. *Ocean Modelling*, *110*, 1–20. https://doi.org/10.1016/J.OCEMOD.2016.12.007

Mao, M., & Xia, M. (2020). Monthly and episodic dynamics of summer circulation in Lake Michigan. *Journal of Geophysical Research: Oceans*, *125*(6). https://doi.org/10.1029/2019jc015932

Mellor, G. L., & Yamada, T. (1982). Development of a turbulence closure model for geophysical fluid problems. *Reviews of Geophysics*, *20*(4), 851. https://doi.org/10.1029/RG020i004p00851
Mengual, B., Hir, P., Cayocca, F., & Garlan, T. (2017). Modelling fine sediment dynamics: Towards a common erosion law for fine sand, mud and mixtures. *Water*, *9*(8), 564. https://doi.org/10.3390/w9080564
Meyer-Peter, E., & Müller, R. (1948). *Formulas for bed-load transport*. IAHSR 2nd Meeting. Retrieved from https://repository.tudelft.nl/islandora/object/uuid%3A4fda9b61-be28-4703-ab06-43cdc2a21bd7
Miller, T. R. (2020). *Lakestat*. Retrieved from http://www.lakestat.com/
Mitchener, H., & Torfs, H. (1996). Erosion of mud/sand mixtures. *Coastal Engineering*, *29*(1–2), 1–25. https://doi.org/10.1016/S0378-3839(96)00002-6
Moore, J. R., Meyer, R. P., & Morgan, C. L. (1973). *Investigation of the sediments and potential manganese nodule resources of Green Bay* (Technical Report-WIS. WISCU-T-73-001). University of Wisconsin, Sea Grant College Program.
Nakano, D., & Strayer, D. L. (2014). Biofouling animals in fresh water: Biology, impacts, and ecosystem engineering on JSTOR. *Frontiers in Ecology and the Environment*, *12*(3), 167–175. https://doi.org/10.1890/130071
National Geophysical Data Center. (2015). *Bathymetric data viewer*. Retrieved from http://maps.ngdc.noaa.gov/viewers/bathymetry/
NEW Water. https://www.newwater.us/programs/aquatic-monitoring
Niu, Q., Xia, M., Ludsin, S. A., Chu, P. Y., Mason, D. M., & Rutherford, E. S. (2018). High-turbidity events in Western Lake Erie during ice-free cycles: Contributions of river-loaded vs. resuspended sediments. *Limnology & Oceanography*, *63*(6), 2545–2562. https://doi.org/10.1002/LNO.10959
NOAA. (2017). *Bathymetry of Lake Michigan*. Retrieved from https://ngdc.noaa.gov/mgg/greatlakes/michigan.html
NOAA. https://www.ncei.noaa.gov/maps/hourly/
NOAA. (2020). *Station selection—NOAA tides & currents*. Retrieved from https://tidesandcurrents.noaa.gov/stations.html?type=Water+Levels
NOAA. (2021a). Lake Michigan and Huron operational forecast system (LMHOFS) information. Retrieved from https://tidesandcurrents.noaa.gov/ofs/lmhofs/lmhofs_info.html
NOAA. (2021b). NOAA/GLERL Great lakes coastal forecasting system, GLCFS. Retrieved from https://www.glerl.noaa.gov/res/glcfs/
Ouillon, S. (2018). Why and how do we study sediment transport? Focus on coastal zones and ongoing methods. *Water*, *10*(4), 390. https://doi.org/10.3390/w10040390
Parker, G. (2004). *1D morphodynamics of rivers and turbidity currents Saint Anthony Falls Lab*. Univ. of Minn., Minneapolis. Retrieved from http://hydrolab.illinois.edu/people/parkerg/morphodynamics_e-book.htm
Qi, J., Chen, C., Beardsley, R. C., Perrie, W., Cowles, G. W., & Lai, Z. (2009). An unstructured-grid finite-volume surface wave model (FVCOM-SWAVE): Implementation, validations and applications. *Ocean Modelling*, *28*(1–3), 153–166. https://doi.org/10.1016/J.OCEMOD.2009.01.007
Qualls, T., Harris, H. J., & Harris, V. (2013). *The state of Green Bay: The condition of the bay of Green Bay/Lake Michigan 2013*. University of Wisconsin Sea Grant Institute. Retrieved from https://www.seagrant.wisc.edu/wp-content/uploads/2018/11/State-of-the-Bay-Report-2013.pdf
Read, J., Klump, V., Johengen, T., Schwab, D., Paige, K., Eddy, S., et al. (2010). Working in freshwater: The Great Lakes observing system contributions to regional and national observations, data infrastructure, and decision support. *Marine Technology Society Journal*, *44*(6), 84–98. https://doi.org/10.4031/MTSJ.44.6.12
Ris, R. C., Holthuijsen, L. H., & Booij, N. (1999). A third-generation wave model for coastal regions: 2. Verification. *Journal of Geophysical Research*, *104*(C4), 7667–7681. https://doi.org/10.1029/1998JC900123
Rowe, M. D., Anderson, E. J., Vanderploeg, H. A., Pothoven, S. A., Elgin, A. K., Wang, J., & Yousef, F. (2017). Influence of invasive quagga mussels, phosphorus loads, and climate on spatial and temporal patterns of productivity in Lake Michigan: A biophysical modeling study. *Limnology & Oceanography*, *62*(6), 2629–2649. https://doi.org/10.1002/lno.10595
Rowe, M. D., Anderson, E. J., Wang, J., & Vanderploeg, H. A. (2015). Modeling the effect of invasive quagga mussels on the spring phytoplankton bloom in Lake Michigan. *Journal of Great Lakes Research*, *41*, 49–65. https://doi.org/10.1016/J.JGLR.2014.12.018
Safaie, A., Wendzel, A., Ge, Z., Nevers, M. B., Whitman, R. L., Corsi, S. R., & Phanikumar, M. S. (2016). Comparative evaluation of statistical and mechanistic models of *Escherichia coli* at beaches in Southern Lake Michigan. *Environmental Science & Technology*, *50*(5), 2442–2449. https://doi.org/10.1021/acs.est.5b05378
Sanford, L. P. (2008). Modeling a dynamically varying mixed sediment bed with erosion, deposition, bioturbation, consolidation, and armoring. *Computers & Geosciences*, *34*(10), 1263–1283. https://doi.org/10.1016/j.cageo.2008.02.011
Schwab, D. J. (1983). Numerical simulation of low-frequency current fluctuations in Lake Michigan. *Journal of Physical Oceanography*, *13*(12), 2213–2224. https://doi.org/10.1175/1520-0485(1983)013<2213:nsolfc>2.0.co;2
Schwab, D. J., & Beletsky, D. (1998). *Lake Michigan mass balance study: Hydrodynamic modeling ProjectERL GLERL-108*. NOAA GLERL. https://www.glerl.noaa.gov/ftp/publications/tech_reports/glerl-108/tm-108.pdf
Shen, C. (2016). *Modeling of dreissenid mussel impacts on Lake Michigan* (ProQuest Dissertations and Theses). University of Wisconsin-Milwaukee. https://dc.uwm.edu/etd/1309/
Sherwood, C. R., Aretxabaleta, A. L., Harris, C. K., Paul Rinehimer, J., Verney, R., & Ferré, B. (2018). Cohesive and mixed sediment in the Regional Ocean Modeling System (ROMS v3.6) implemented in the Coupled Ocean-Atmosphere-Wave-Sediment Transport Modeling System (COAWST r1234). *Geoscientific Model Development*, *11*(5), 1849–1871. https://doi.org/10.5194/gmd-11-1849-2018
Shore, J. A. (2009). Modelling the circulation and exchange of Kingston Basin and Lake Ontario with FVCOM. *Ocean Modelling*, *30*(2–3), 106–114. https://doi.org/10.1016/J.OCEMOD.2009.06.007
Smagorinsky, J. (1963). General circulation experiments with the primitive equations, I. The basic experiment. *Monthly Weather Review*, *91*(3), 99–164. https://journals.ametsoc.org/view/journals/mwre/91/3/1520-0493_1963_091_0099_gcewtp_2_3_co_2.xml
Soulsby, R. L. (1998). *Dynamics of marine sands*. https://eprints.hrwallingford.com/412/
Valipour, R., Boegman, L., Bouffard, D., & Rao, Y. R. (2017). Sediment resuspension mechanisms and their contributions to high-turbidity events in a large lake. *Limnology & Oceanography*, *62*(3), 1045–1065. https://doi.org/10.1002/LNO.10485
Valipour, R., León, L. F., Depew, D., Dove, A., & Rao, Y. R. (2016). High-resolution modeling for development of nearshore ecosystem objectives in eastern Lake Erie. *Journal of Great Lakes Research*, *42*(6), 1241–1251. https://doi.org/10.1016/J.JGLR.2016.08.011
Velleux, M., Endicott, D., Steuer, J., Jaeger, S., & Patterson, D. (1995). Long-term simulation of PCB export from the Fox River to Green Bay. *Journal of Great Lakes Research*, *21*(3), 359–372. https://doi.org/10.1016/S0380-1330(95)71047-4
Waples, J. T., & Klump, J. V. (2002). Biophysical effects of a decadal shift in summer wind direction over the Laurentian Great Lakes. *Geophysical Research Letters*, *29*(8), 431–434. https://doi.org/10.1029/2001GL014564

Warner, J. C., Sherwood, C. R., Signell, R. P., Harris, C. K., & Arango, H. G. (2008). Development of a three-dimensional, regional, coupled wave, current, and sediment-transport model. *Computers & Geosciences*, *34*(10), 1284–1306. https://doi.org/10.1016/J.CAGEO.2008.02.012

Wisconsin DNR. (2000). *Model evaluation workgroup technical memorandum 2f: Estimation of sediment bed properties for Green Bay*.

Wolanski, E. (2007). Estuarine sediment dynamics. In *Estuarine ecohydrology* (pp. 41–69). Elsevier. https://doi.org/10.1016/b978-044453066-0.50004-0

Wolanski, E., & Elliott, M. (2015). *Estuarine ecohydrology: An introduction*. Elsevier. https://doi.org/10.1016/c2013-0-13014-0

Wyrtki, K. (1965). The average annual heat balance of the North Pacific Ocean and its relation to ocean circulation. *Journal of Geophysical Research*, *70*(18), 4547–4559. https://doi.org/10.1029/JZ070I018P04547

Xue, P., Schwab, D. J., & Hu, S. (2015). *An investigation of the thermal response to meteorological forcing in a hydrodynamic model of Lake Superior*. Retrieved from https://www.semanticscholar.org/paper/An-investigation-of-the-thermal-response-to-forcing-Xue-Schwab/40eca7b276ebcad8589f9df017dbd724b1ffc00d

Yolcubal, I., Brusseau, M. L., Artiola, J. F., Wierenga, P., & Wilson, L. G. (2004). Environmental physical properties and processes. *Environmental Monitoring and Characterization*, 207–239. https://doi.org/10.1016/B978-012064477-3/50014-X

Zhang, J., Xiong, M., Yin, C., & Gan, S. (2018). Inner shelf response to storm track variations over the east LeiZhou Peninsula, China. *International Journal of Applied Earth Observation and Geoinformation*, *71*, 56–69. https://doi.org/10.1016/J.JAG.2018.03.011